

Evidence for weak deformation in the 88-neutron nucleus $^{153}\text{Tb}^\dagger$

M. D. Devous, Sr.,* and T. T. Sugihara

Cyclotron Institute, Texas A&M University, College Station, Texas 77843

(Received 15 January 1976)

The decay of 6.3-h ^{153}Dy to levels in ^{153}Tb has been studied with high-resolution detectors. Sources were prepared by the $^{154}\text{Gd}(^3\text{He}, 4n)$ reaction and chemically purified by ion exchange. A total of 329 γ rays were assigned to ^{153}Dy decay; another 71 γ rays may be associated with ^{153}Dy decay. The proposed decay scheme of 54 levels includes 319 of the 400 γ rays. The Q value for β decay was measured to be 2250 ± 50 keV. Eleven low-lying positive-parity levels were interpreted in the Coriolis-mixed, particle-plus-rotor model as Nilsson states and rotational band members. Nilsson orbitals so interpreted include $5/2^+[402]$, ground state; $3/2^+[411]$, 147.4 keV; $5/2^+[413]$, 218.6 keV; and $7/2^+[404]$, 254.2 keV. The order and spacing of the negative-parity levels are consistent with rotation-alignment model predictions. For both positive- and negative-parity levels a deformation β of about 0.15 is required to fit the data.

RADIOACTIVITY ^{153}Dy [from $^{154}\text{Gd}(^3\text{He}, 4n)$]; measured E_γ , I_γ , I_{ce} , Q_β , γ - γ , and β^+ - γ coin; deduced α_k , $\log ft$. ^{153}Tb deduced levels, J, π . Enriched target, Ge(Li) and Si(Li) detectors.

I. INTRODUCTION

Experimental information about transitional nuclei between the closed shell at $N = 82$ and the stably deformed region at $N = 90$ is rapidly accumulating. Much of the new data, however, is concerned with high-spin states in even-even nuclei¹ and with shape coexistence in odd- N nuclei.² Studies of proton transfer in $(^3\text{He}, d)$ and (α, t) reactions on Gd target nuclei³ have identified proton states in well-deformed Tb nuclei ($^{155}\text{Tb}_{90}$ and heavier), but for the lighter Tb nuclei, excited states have not been well characterized. No quantitatively adequate description of proton states in the region of soft nuclei presently exists.

In this paper we report the results of a detailed study of levels in the $N = 88$ nucleus ^{153}Tb as populated in the decay of 6.3-h ^{153}Dy . Two fairly detailed cases of ^{153}Dy decay have been reported. In the conversion-electron study by Harmatz and Handley⁴ 84 transitions were placed among 21 levels (their paper contains references to the earlier literature). Very recently, while our work was in progress, Zuber *et al.*⁵ reported a study in which more than 250 transitions were assigned to ^{153}Dy decay. Zuber *et al.* reported 14 levels which were in agreement with those proposed by Harmatz and Handley; they proposed 38 additional levels. Simultaneous with our work a reaction study of the $N = 88$ nuclei ^{149}Pm , ^{151}Eu , and ^{153}Tb has recently been completed.⁶ We assign 400 transitions to ^{153}Tb decay; 54 levels are identified in ^{153}Tb , 33 below 1 MeV.

Both Harmatz and Handley⁴ and Zuber *et al.*⁵ interpreted the $5/2^+$ ground state, the 80.8-keV $7/2^+$

state, and the $11/2^-$ isomeric state as the $d_{5/2}$, $g_{7/2}$, and $h_{11/2}$ shell-model states, respectively. In addition, Zuber *et al.* proposed that states at 147.4, 240.5, 389.6, and 572.1 keV were members of a $3/2^+[411]$ rotational band. Earlier studies⁷ of ^{151}Eu by the $^{153}\text{Eu}(p, t)$ and the $^{150}\text{Sm}(^3\text{He}, d)$ reactions suggest that the ground state of ^{151}Eu is spherical and that ^{151}Eu has both spherical and deformed excited states. In the $(^3\text{He}, d)$ and (α, t) reaction studies leading to levels in ^{153}Tb , Straume, Løvnhøiden, and Burke⁶ indicate that the shell model is inadequate to explain observed levels and spectroscopic factors and they suggest a possible interpretation of these levels in terms of the Nilsson model with a relatively small deformation. In our study we find that most of the low-lying positive- and negative-parity states can be accounted for by the particle-plus-rotor model with the inclusion of Coriolis mixing.

II. EXPERIMENTAL METHODS AND RESULTS

A. Source preparation

Sources of 6.3-h ^{153}Dy were prepared by irradiation of 2–4 mg of Gd_2O_3 , enriched to 99% in ^{154}Gd , with ^3He ions from the Texas A & M variable energy cyclotron. Typical irradiations were carried out with 1–3 μA of 35-MeV ^3He ions for 30 min. The powdered target material was contained in Al foil. After irradiation, the Gd_2O_3 was dissolved and a carrier-free Dy fraction was separated by ion exchange. Very small quantities of 9.6-h ^{155}Dy and the isomers of ^{154}Tb (8.5 h, 22 h, 23 h) were observed as contaminants of the ^{153}Dy sources. Several hours after the chemical separa-

tion, γ rays from the daughter nucleus 2.3-d ^{153}Tb were also observable.

In preliminary experiments ^3He irradiations were carried out at 30, 35, 40, and 45 MeV in order to determine the optimum bombarding energy and to assign observed γ rays to the proper nuclide. The decay of many γ rays was followed for 24 h. The combination of excitation function and half-life made the assignment of γ rays to ^{153}Dy unambiguous generally for transitions of intensity greater than 1% of the intensity of the 254.2-keV line.

B. γ -ray and β^+ spectra

1. Singles γ -ray experiments

The 8192-channel γ -ray singles spectra were obtained on two Ge(Li) detectors. Detector A (coaxial, 35 cm³, resolution 1.8 keV at 1332 keV) was used for the energy range 80–2500 keV and detector B (planar, 2.0 cm² × 6.7 mm, resolution 0.58 keV at 122 keV) for the energy range 10–400 keV. Sources were counted in a variety of geometries, with and without absorbers, on both counters in order to correct for summing. Typical spectra are shown in Fig. 1.

Analysis of spectra was carried out by a combination of computer and hand analyses. Background stripping was performed by computer and multiplets were resolved by hand plotting. The 400 transitions assigned to the decay of ^{153}Dy are listed in Table I. Some of the intensities were obtained from the analysis of coincidence spectra for multiplets not resolvable in singles spectra. No transitions of energy below 70 keV were found. Weak lines of energy similar to x-ray energies, however, would not have been detected. The 511.9-keV transition could be resolved from annihilation radiation in the singles spectra; its intensity, however, was better obtained from coincidence spectra.

In general the intensities reported here agree with those of Zuber *et al.*⁵ if experimental errors are taken into account. Two significant discrepancies involve the 82.5- and 444.7-keV γ rays. Our relative intensities are 100 ± 10 and 150 ± 40 for these γ rays, while in Ref. 5 they are reported to be 155 ± 15 and 85 ± 8 .

2. Coincidence experiments

Coincidence experiments were performed with three different pairs of detectors. In each case data were taken in a three-parameter event mode on a PDP 15/40 computer. Each event consisted of the pulse heights from the two detectors and the time between the pulses. A timing pulse from each detector was obtained with a constant

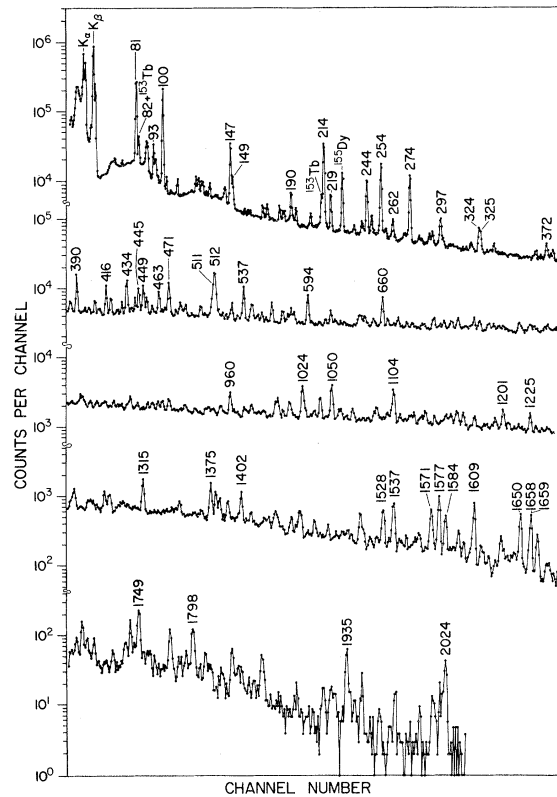


FIG. 1. Typical spectrum of γ rays from the decay of 6.3-h ^{153}Dy . Below 380 keV, a planar Ge(Li) detector was used and for higher energies a coaxial Ge(Li) detector. Only relatively strong lines have been labeled by their energy in keV to indicate the energy scale.

fraction discriminator and these pulses were used to start and stop a time-to-amplitude converter. A Tennelec PACE system was used to digitize the pulse-height and time information.

Detector pairs used in $\gamma\gamma$ experiments included (1) detector A and a second Ge(Li) detector of nearly the same efficiency and slightly poorer resolution and (2) detectors A and B. 180° counting geometry was employed. True-to-random ratios were typically 80 to 1. The resolving time, full width at half maximum (FWHM), was typically 12 nsec. In coincidence experiment (1), 3×10^7 events were recorded in the energy range 100–2000 keV. In experiment (2), 1.8×10^7 events were recorded and the lower energy limit in detector B was about 60 keV.

The raw data were divided into prompt and random events. For this purpose the prompt time window was set to be 38 nsec, corresponding to the full width at $\frac{1}{20}$ of the maximum of the time resolution curve. The events were sorted into an ordered array of spectra according to the methods of Haenni.⁸ Gates were set on essentially every

TABLE I. Energies and intensities of γ rays observed in the decay of 6.3-h ^{153}Dy and their placement in the level scheme of ^{153}Tb .

| E_γ (keV) | I_γ ^a | Assignment | | E_γ (keV) | I_γ ^a | Assignment | |
|-----------------------|-------------------------|---------------------------|-------------------------|-----------------------|-------------------------|---------------------------|-------------------------|
| | | Initial level (keV) | Final level (keV) | | | Initial level (keV) | Final level (keV) |
| 70.8(1) | 9(2) ^b | 325.0 | 254.2 ^c | 296.0(2) | 23(5) ^b | 740.7 | 444.7 ^c |
| 71.1(1) | 4(2) ^b | 218.6 | 147.4 ^c | 296.6(1) | 140(14) ^b | 510.4 ^c | 213.8 ^c |
| 78.4(2) ^d | 8(3) | | | 297.6(2) | 22(3) | 957.6 ^c | 660.1 |
| 80.82(5) | 1410(70) | 80.8 ^c | 0 | 299.5(4) | 8(3) | 960.0 | 660.1 |
| 82.5(1) | 100(10) | 163.3 | 80.8 ^c | 302.6(2) | 24(5) | 543.3 | 240.5 ^c |
| 88.1(2) | 23(3) | 660.1 | 571.8 ^c | 305.6(3) | 15(2) | 630.4 | 325.0 |
| 88.9(2) | 42(5) | | | 306.2(5) ^d | 5(2) | 957.6 | 651.7 |
| 93.06(4) | 118(6) | 240.5 ^c | 147.4 ^c | 308.7(2) | 7(10) | 389.6 | 80.8 ^c |
| 94.3(2) | 30(3) | | | 317.5(2) | 19(2) | 571.8 | 254.2 ^c |
| 94.9(2) | 44(4) | | | 323.8(1) | 145(15) | 537.5 ^c | 213.8 ^c |
| 96.0(2) ^d | 9(3) | | | 325.0(1) | 80(10) | 325.0 ^c | 0 |
| 96.7(2) ^d | 9(3) | | | 326.6(3) ^d | 9(3) | 651.7 | 325.0 |
| 99.71(5) | 1260(90) | 263.0 ^c | 163.3 | 331.6(2) | 15(2) | 571.8 | 240.5 ^c |
| 124.4(2) ^d | 14(3) | | | 332.9(2) | 9(2) | 522.4 | 389.6 ^c |
| 125.0(2) | 27(3) | 722.4 | 597.5 ^c | 334.5(1) | 25(3) | 597.5 ^c | 263.0 ^c |
| 127.2(1) | 38(2) | | | 335.1(2) | 10(2) | 660.1 | 325.0 ^c |
| 128.2(1) | 34(2) | 725.6 | 597.5 ^c | 337.4(2) | 11(2) | 726.9 | 389.6 ^c |
| 133.0(1) | 32(2) | 213.8 ^c | 80.8 ^c | 340.6(4) ^d | 3(1) | 1130.9 | 790.1 |
| 143.4(2) | 20(3) | 740.8 | 597.5 | 350.9(2) ^d | 6(1) | 722.4 | 371.6 |
| 144.2(2) | 30(4) | | | 362.0(4) ^d | 2(1) | 1791.4 | 1429.6 |
| 147.44(5) | 420(30) | 147.4 ^c | 0 | 363.0(3) ^d | 4(2) | 510.4 | 147.4 |
| 149.0(1) | 95(10) | 389.6 ^c | 240.5 ^c | 363.9(1) | 40(5) | 444.7 ^c | 80.8 |
| 157.6(2) | 14(2) | 371.6 | 213.8 ^c | 365.9(2) | 5(2) | 529.5 | 163.3 |
| 159.7(3) | 7(2) | 240.5 ^c | 80.8 | 367.4(4) | 8(2) | 630.4 | 263.0 |
| 162.8(5) ^d | 3(2) | 1151.3 | 989.1 | 368.9(4) | 8(2) | 740.7 | 371.6 |
| 173.3(1) | 42(3) | 254.2 ^c | 80.8 ^c | 370.3(2) ^d | 9(2) | | |
| 182.4(2) | 32(3) | 571.8 ^c | 389.6 ^c | 371.6(1) | 98(8) | 371.6 | 0 |
| 185.4(2) | 15(2) ^b | 510.4 | 325.0 ^c | 374.2(1) | 22(5) | | |
| 185.7(2) | 9(2) ^b | 630.4 | 444.7 ^c | 376.1(1) } | | 1365.2 | 989.1 |
| 188.5(5) ^d | 6(3) | | | 376.2(1) } | 40(6) | 630.4 | 254.2 ^c |
| 190.5(1) | 110(6) | 444.7 ^c | 254.2 ^c | 378.4(3) ^d | 6(2) | 1151.3 | 772.8 |
| 191.9(4) | 9(4) | 1429.6 | 1238.0 | 383.6(2) | 25(3) | 597.5 | 213.8 ^c |
| 193.8(1) | 47(5) | 1151.3 | 957.6 ^c | 384.7(2) | 15(3) | | |
| 204.3(2) | 35(6) | 529.5 ^c | 325.0 ^c | 389.61(7) | 165(8) | 389.6 ^c | 0 |
| 209.9(2) | 17(4) | 807.6 | 597.5 | 395.9(2) | 11(4) | 543.5 | 147.4 ^c |
| 213.77(5) | 1320(60) | 213.8 ^c | 0 | 397.5(2) | 11(2) | 651.7 | 254.2 ^c |
| 218.6(1) | 175(10) | 218.6 ^c | 0 | 400.7(2) | 14(2) | 725.6 | 325.0 ^c |
| 235.4(1) | 24(3) | 772.8 ^c | 537.5 ^c | 403.8(4) ^d | 3(2) | 1130.9 | 726.9 |
| 240.5(1) | 43(3) | 240.5 ^c | 0 | 405.9(1) | 50(5) | 660.1 | 254.2 ^c |
| 242.0(2) | 16(2) | 389.6 ^c | 147.4 ^c | 408.7(4) | 14(4) | 1130.9 | 722.4 |
| 244.25(5) | 480(30) | 325.0 ^c | 80.8 ^c | 410.8(4) | 10(3) | 651.7 | 240.5 ^c |
| 247.4(1) | 60(5) | 510.4 ^c | 263.0 ^c | 415.75(6) | 130(15) | 740.7 | 325.0 ^c |
| 254.23(5) | $\equiv 1000$ | 254.2 ^c | 0 | 419.0(3) | 8(2) | 1226.5 | 807.6 |
| 258.0(3) | 25(5) | | | 420.1(1) | 65(8) | 957.6 ^c | 537.5 ^c |
| 260.9(5) ^d | 5(3) | 790.1 | 529.5 | 424.6(4) | 4(1) | | |
| 262.4(1) | 110(25) | 799.9 | 537.5 ^c | 425.9(3) | 13(3) | 1791.4 | 1365.2 |
| 264.0(4) ^d | 6(3) | 807.6 | 543.5 | 429.6(1) | 33(5) | 510.4 | 80.8 |
| 269.8(3) ^d | 7(3) | 510.4 | 240.5 | 434.2(1) | 160(20) | 597.5 ^c | 163.3 |
| 271.0(2) | 22(4) | 799.9 | 529.5 | 438.2(2) | 18(3) | 651.7 | 213.8 ^c |
| 272.3(2) | 21(3) | 597.5 ^c | 325.0 | 441.6(1) | 44(5) | 660.1 | 218.6 ^c |
| 274.5(1) | 830(40) | 537.5 ^c | 263.0 ^c | 444.7(1) | 150(40) | 444.7 ^c | 0 |
| 281.2(2) | 25(3) | 725.6 | 444.7 ^c | 448.8(1) | 130(15) | 529.5 ^c | 80.8 ^c |
| 283.1(2) | 16(3) | 537.5 | 254.2 ^c | 451.6(1) | 57(4) | 989.1 | 537.5 ^c |
| 289.0(1) | 27(7) | 543.5 | 254.2 ^c | 456.7(1) | 23(5) | 537.5 | 80.8 ^c |
| 290.8(1) | 67(4) | 371.6 | 80.8 ^c | 462.6(1) | 95(14) | 725.6 | 263.0 ^c |
| 295.5(1) | 21(4) | | | 465.8(2) | 15(3) | 1238.0 | 772.8 ^c |

TABLE I (Continued)

| E_γ (keV) | I_γ^a | Assignment | | E_γ (keV) | I_γ^a | Assignment | |
|-----------------------|--------------|---------------------------|-------------------------|-----------------------|--------------|---------------------------|-------------------------|
| | | Initial level (keV) | Final level (keV) | | | Initial level (keV) | Final level (keV) |
| 467.7(2) | 10(2) | 1240.5 | 772.8 | 654.8(3) | 10(2) | 1226.5 | 571.8 |
| 468.7(2) | 26(4) | | | 657.7(3) | 9(2) | | |
| 471.4(1) | 150(8) | 725.6 | 254.2 ^c | 660.0(1) | 140(20) | 740.8 | 80.8 ^c |
| 473.6(4) ^d | 7(2) | | | 673.8(2) | 33(3) | 1824.9 | 1151.3 |
| 477.9(2) | 24(3) | | | 681.5(2) | 20(3) | 1341.4 | 660.1 |
| 480.6(2) | 44(5) | | | 685.7(2) | 14(2) | 1912.5 | 1226.5 |
| 482.0(2) | 26(3) | 722.4 | 240.5 ^c | 686.3(4) | 9(3) | 1130.9 | 444.7 |
| 485.7(1) | 40(5) | 1226.5 | 740.8 | 695.0(4) | 12(3) | 1238.0 | 543.5 |
| 491.2(3) | 15(4) | { 571.8 | 80.8 | 697.4(3) | 16(3) | 1226.5 | 529.5 |
| 500.0(1) | 35(5) | { 1151.3 | 660.1 | 704.0(1) | 32(5) | 1429.6 | 725.6 |
| 503.6(3) | 11(4) | 740.8 | 240.5 ^c | 705.8(1) | 70(20) | 960.0 | 254.2 ^c |
| 508.8(4) | 40(7) | 722.4 | 218.6 | 709.0(4) | 8(2) | { 1238.0 | 529.5 |
| 511.9(1) | 290(40) | 722.4 ^c | 213.8 ^c | 711.0(4) | 15(4) | { 790.0 | 80.8 |
| 513.1(1) | 75(10) | 726.9 ^c | 213.8 ^c | 714.0(2) | 28(4) | 1341.4 | 630.4 |
| 514.9(3) | | 1240.5 | 725.6 ^c | 719.4(2) | 10(3) | 960.0 | 240.5 ^c |
| 515.6(3) | 26(8) | 1238.0 | 722.4 ^c | 722.2(2) | 30(6) | 722.4 | 0 |
| 518.6(2) ^d | 18(3) | | | 725.6(2) | 14(3) | | |
| 522.0(3) | 16(3) | 740.8 | 218.6 ^c | 726.9(1) | 30(10) | 726.9 | 0 |
| 525.5(2) | 9(3) | | | 740.8(1) | 36(6) | 740.8 | 0 |
| 527.3(2) | 64(5) | 790.1 ^c | 263.0 ^c | 744.8(2) | 14(2) | | |
| 532.7(3) | 17(4) | 772.8 | 240.5 | 746.2(2) | 28(4) | 960.0 | 213.8 ^c |
| 535.8(1) | 23(3) | 790.1 | 254.2 ^c | 752.9(4) | 22(6) | 1836.0 | 1083.3 |
| 537.5(1) | 150(25) | 537.5 ^c | 0 | 754.6(4) | 22(6) | | |
| 543.2(2) | 30(6) | 543.5 | 0 | 758.3(3) | 18(2) | 1083.3 | 325.0 ^c |
| 544.8(1) | 60(8) | 807.6 | 263.0 ^c | 762.0(3) | 22(4) | 1151.3 | 389.6 |
| 553.4(1) | 30(7) | 807.6 | 254.2 ^c | 766.2(3) | 16(3) | | |
| 557.6(2) ^d | 9(2) | 1365.2 | 807.6 | 779.9(2) | 32(5) | 1151.3 | 371.6 |
| 562.3(1) | 70(10) | 725.6 | 163.3 | 781.6(2) | 19(3) | 1226.5 | 444.7 |
| 570.9(3) | 13(3) | 1912.5 | 1341.4 | 783.9(2) | 14(3) | 2024.2 | 1240.5 |
| 571.8(1) | 40(6) | 571.8 | 0 | 785.6(4) ^d | 3(2) | 2011.9 | 1226.5 |
| 574.1(4) ^d | 8(3) | 1939.8 | 1365.2 | 788.4(3) | 12(3) | 1939.8 | 1151.1 |
| 576.3(2) | 26(6) | 790.1 | 213.8 ^c | 790.0(2) | 20(4) | 790.1 | 0 |
| 579.3(1) | 55(5) | 726.9 ^c | 147.4 ^c | 793.3(2) | 18(3) | { 1365.2 | 571.8 |
| 581.0(3) | 13(3) | 799.9 | 218.6 ^c | | | { 1238.0 | 444.7 |
| 582.2(2) | 45(8) | 2011.9 | 1429.6 | 796.0(4) ^d | 5(2) | 1240.5 | 444.7 |
| 593.8(1) | 140(15) | 807.6 | 213.8 ^c | 802.4(3) | 10(3) | 1762.2 | 960.0 |
| 597.4(2) ^d | 12(3) | | | 804.8(2) | 21(4) | 1762.2 | 957.6 |
| 601.0(5) ^d | 3(2) | 1130.9 | 529.5 | 820.4(2) | 18(3) | 1083.3 | 263.0 |
| 604.6(5) ^d | 8(3) | | | 827.7(2) | 35(4) | 1365.2 | 537.5 ^c |
| 609.5(1) | 21(4) | 1836.0 | 1226.5 | 829.6(3) | 30(4) | 1083.3 | 254.2 ^c |
| 610.9(2) ^d | 8(2) | 1762.2 | 1151.3 | 831.4(2) | 22(3) | 1791.4 | 960.0 |
| 614.3(1) | 60(6) | 1341.4 | 726.9 ^c | 836.0(2) | 15(3) | { 1824.9 | 989.1 |
| 618.6(2) | 16(3) | | | | | { 1365.2 | 529.5 |
| 623.1(4) ^d | 7(2) | | | 841.7(2) | 14(4) | 989.1 | 147.4 |
| 626.5(4) | 7(2) | 790.1 | 163.3 | 843.0(3) | 22(4) | 1083.3 | 240.5 |
| 635.3(4) ^d | 7(2) | 960.0 | 325.0 | 846.4(2) | 11(3) | 1836.0 | 989.1 |
| 637.3(4) ^d | 5(2) | | | 848.7(3) | 17(3) | 1238.0 | 389.6 |
| 638.1(3) | 15(5) | 1365.2 | 726.9 ^c | 850.8(3) | 16(4) | 1240.5 | 389.6 |
| 640.0(3) | 38(5) | 1365.2 | 725.6 ^c | 857.7(2) | 22(3) | 1429.6 | 571.8 |
| 641.5(3) | 11(2) | 722.4 | 80.8 | 864.4(3) | 16(3) | 1083.3 | 218.6 |
| 643.2(3) | 11(3) | 1240.5 | 597.5 | 869.5(2) | 14(3) | 1083.3 | 213.8 |
| 644.5(2) | 38(6) | 807.6 | 163.3 | 871.5(2) | 38(4) | | |
| 647.0(4) | 7(2) | 2011.9 | 1365.2 | 873.0(3) | 16(3) | | |
| 652.7(3) | 26(5) | 799.9 | 147.4 ^c | 878.9(2) | 18(4) | 960.0 | 80.8 |
| 653.4(3) | 12(3) | | | 886.3(2) | 22(3) | 1429.5 | 543.5 |

TABLE I (Continued)

| E_γ (keV) | I_γ ^a | Assignment | | E_γ (keV) | I_γ ^a | Assignment | |
|------------------------|-------------------------|------------------------------|---------------------------|------------------------|-------------------------|---------------------------|-------------------------|
| | | Initial level (keV) | Final level (keV) | | | Initial level (keV) | Final level (keV) |
| 891.8(2) | 20(3) | 1429.6 | 537.5 ^c | 1132.7(2) | 24(4) | 1858.3 | 725.6 |
| 896.5(3) | 24(4) | 1341.4 | 444.7 | 1140.3(3) | 22(4) | 1939.8 | 799.9 |
| 900.4(2) | 26(3) | 1429.6 | 529.5 ^c | 1142.0(5) ^d | 6(3) | | |
| 920.0(2) | 21(3) | 1083.3 | 163.3 | 1147.5(5) ^d | 5(3) | | |
| 921.9(3) ^d | 8(3) | | | 1151.2(2) | 26(4) | 1365.2 | 213.8 ^c |
| 928.8(3) ^d | 7(2) | 2011.9 | 1083.3 | 1153.5(4) | 11(3) | | |
| 937.6(2) | 9(3) | 1151.3 | 213.8 | 1159.0(5) ^d | 7(3) | | |
| 939.4(2) | 18(3) | | | 1161.0(2) | | 1791.4 | 630.4 |
| 941.5(2) | 22(4) | | | 1161.1(2) | 34(5) | 2121.1 | 960.0 |
| 944.2(2) | 18(3) | | | 1166.5(3) | 20(4) | 1429.6 | 263.0 ^c |
| 945.8(3) | 11(3) | | | 1175.6(3) | 10(4) | 1429.6 | 254.2 ^c |
| 950.9(2) | 26(5) | 1939.8 | 989.1 | 1176.0(3) | 19(4) | 1836.0 | 660.1 |
| 952.7(2) | 18(3) | 1912.5 | 960.0 | 1183.8(4) ^d | 5(2) | | |
| 954.4(4) ^d | 7(3) | 1762.2 | 807.6 | 1185.7(4) ^d | 6(2) | 1912.5 | 726.9 |
| 960.0(2) | 80(20) | 960.0 | 0 | 1187.2(4) ^d | 6(2) | 1912.5 | 725.6 |
| 963.4(2) | 16(3) | 1226.5 | 263.0 | 1191.4(4) ^d | 8(3) | | |
| 966.1(2) | 14(2) | | | 1194.2(3) | 26(4) | 1341.4 | 147.4 |
| 972.4(2) | 28(4) | 1226.5 | 254.2 ^c | 1199.4(4) | 15(3) | 1939.8 | 740.8 |
| 974.3(3) | 10(3) | | | 1201.5(2) | 55(8) | 1365.2 | 163.3 |
| 978.2(3) | 12(3) | | | 1206.1(3) | 21(4) | 1836.0 | 630.4 |
| 979.7(2) | 35(4) | 1939.8 | 960.0 | 1210.6(5) ^d | 3(2) | 1429.6 | 218.6 |
| 989.4(4) | 6(2) | 989.1 | 0 | 1215.0(3) | 20(4) | 1429.6 | 213.8 |
| 1000.0(3) | 8(3) | 1240.5 | 240.5 ^c | 1217.5(5) ^d | 3(2) | 1939.8 | 722.4 |
| 1002.5(1) | 65(10) | 1083.3 | 80.8 ^c | 1225.1(2) | 55(7) | 1822.7 | 597.5 ^c |
| 1006.8(3) | 14(4) | 1779.4 | 772.8 | 1230.4(4) | 10(3) | | |
| 1012.7(1) | 55(5) | 1226.5 | 213.8 ^c | 1252.0(3) | 17(3) | 1762.2 | 510.4 |
| 1014.2(2) | 20(4) | | | 1254.0(2) | 55(7) | 1791.4 | 537.5 ^c |
| 1015.7(5) ^d | 4(2) | 1822.7 | 807.6 | 1266.0(3) | 13(3) | 1429.6 | 163.3 |
| 1024.2(1) | 130(20) | 1238.0 | 213.8 ^c | 1268.1(3) | 17(4) | | |
| 1026.7(2) | 25(6) | 1240.5 | 213.8 ^c | 1270.1(3) | 15(4) | | |
| 1031.2(3) | 16(4) | | | 1271.6(3) | 16(4) | 2011.9 | 740.8 |
| 1033.7(4) | 11(3) | | | 1274.2(4) | 11(3) | | |
| 1035.3(2) | 30(4) | 1762.2 | 726.9 | 1279.4(4) | 9(3) | 1822.7 | 543.5 |
| 1040.0(2) | 20(5) ^b | 1429.6 | 389.6 ^c | 1281.1(2) | 50(10) | 1791.4 | 510.4 |
| 1040.2(1) | 75(16) ^b | 1365.2 | 325.0 ^c | 1284.2(3) | 25(4) | 1365.2 | 80.8 |
| 1050.1(1) | 170(20) | 1130.9 | 80.8 ^c | 1285.3(3) | 35(6) | 2011.9 | 726.9 |
| 1056.8(2) | 30(4) | 1779.4 | 722.4 | 1287.2(4) | 9(3) | 1824.9 | 537.5 |
| 1058.5(2) | 25(4) | 1858.3 | 799.9 | 1293.3(3) | 11(3) | 1822.7 | 529.5 |
| 1062.7(2) | 27(4) | | | 1295.7(2) | 22(4) | 1824.9 | 529.5 |
| 1068.4(2) | 24(4) | 1858.2 | 790.1 | 1297.6(3) | 19(3) | 2024.2 | 726.9 |
| 1075.5(5) ^d | 6(3) | 1238.0 | 163.3 | 1299.8(5) ^d | 6(3) | 2024.2 | 725.6 |
| 1077.6(4) ^d | 9(3) | | | 1301.5(3) | 16(3) | 2024.2 | 722.4 |
| 1082.3(4) ^d | 8(3) | 1822.7 | 740.8 | 1306.3(3) | 15(3) | 1836.0 | 529.5 |
| 1087.4(2) | 29(4) | 1341.4 | 254.2 ^c | 1308.4(4) ^d | 8(3) | | |
| 1096.8(4) | 9(3) | 1822.7 | 725.6 | 1310.2(4) | 10(3) | 1939.8 | 630.4 |
| 1099.3(2) | 25(4) | 1824.9 | 725.6 | 1315.0(1) | 100(15) | 1912.5 | 597.5 ^c |
| 1102.5(2) | 30(4) | { 1365.2 1824.9 | { 263.0 722.4 | 1325.6(4) ^d | 5(2) | 1836.0 | 510.4 |
| 1104.6(1) | 130(20) | 1429.6 | 325.0 ^c | 1340.5(4) | 9(3) | 1912.5 | 571.8 |
| 1110.9(2) | 20(4) | 1365.2 | 254.2 ^c | 1344.6(4) ^d | 7(3) | | |
| 1118.1(3) | 14(4) | 1858.3 | 740.8 | 1347.6(3) | 27(5) | 1858.3 | 510.4 ^c |
| 1119.6(3) | 21(4) | 1779.4 | 660.1 | 1375.0(1) | 90(15) | 1912.5 | 537.5 ^c |
| 1122.5(2) | 29(4) | 1912.5 | 790.1 ^c | 1380.2(2) | 80(20) | 1824.9 | 444.7 ^c |
| 1129.0(2) | 21(4) | | | 1383.1(3) | 50(10) | 1912.5 | 529.5 ^c |
| | | | | 1389.8(2) | 35(7) | 1779.4 | 389.6 ^c |
| | | { 1858.3 1791.4 1762.2 | { 726.9 660.1 630.4 | 1399.0(4) | 9(3) | 2121.1 | 722.4 |
| 1131.5(3) | 20(4) | | | 1402.1(2) | 79(8) | 1912.5 | 510.4 ^c |

TABLE I (Continued)

| E_γ (keV) | I_γ ^a | Assignment | | E_γ (keV) | I_γ ^a | Assignment | |
|------------------------|-------------------------|---------------------------|-------------------------|------------------------|-------------------------|---------------------------|-------------------------|
| | | Initial level (keV) | Final level (keV) | | | Initial level (keV) | Final level (keV) |
| 1410.6(2) | 13(3) | 1939.8 | 529.5 ^c | 1608.9(2) | 85(18) | 1822.7 | 213.8 ^c |
| 1422.6(4) | 9(3) | | | 1615.2(4) | 13(4) | 1939.8 | 325.0 ^c |
| 1426.5(5) | 7(3) | 2024.2 | 597.5 | 1617.6(5) ^d | 5(2) | 1858.3 | 240.5 |
| 1431.1(3) | 19(4) | | | 1622.4(5) ^d | 4(2) | 2011.9 | 389.6 |
| 1433.1(2) | 22(4) | 1822.7 | 389.6 ^c | 1627.8(5) ^d | 4(2) | 1791.4 | 163.3 |
| 1446.4(3) | 21(4) | 1836.0 | 389.6 ^c | 1632.9(3) | 28(7) | | |
| 1453.3(3) | 26(4) | 1824.9 | 371.6 | 1637.7(5) ^d | 5(2) | | |
| 1454.8(3) | 30(5) | 1779.4 | 325.0 ^c | 1645.0(5) ^d | 4(2) | 1858.3 | 213.8 |
| 1461.1(4) | 11(4) | 2121.1 | 660.1 | 1649.5(2) | 50(15) | 1912.5 | 263.0 ^c |
| 1466.6(3) | 23(4) | 1791.4 | 325.0 ^c | 1658.3(2) | 35(10) | 1912.5 | 254.2 ^c |
| 1467.8(3) | | 1912.5 | 444.7 ^c | 1659.3(2) | 25(8) | 1822.7 | 163.3 |
| 1486.6(4) | 8(3) | 1858.3 | 371.6 | 1672.2(5) | 6(3) | 1912.5 | 240.5 |
| 1495.1(5) ^d | 4(2) | 1939.8 | 444.7 | 1675.8(5) | 9(3) | | |
| 1497.3(5) | 7(3) | 1822.7 | 325.0 | 1694.1(5) ^d | 4(2) | 1912.5 | 218.6 |
| 1500.0(5) ^d | 4(2) | | | 1699.3(4) | 15(4) | 1912.5 | 213.8 |
| 1508.0(2) | 45(10) | 1762.2 | 254.2 ^c | 1710.8(5) ^d | 4(2) | 1858.3 | 147.4 |
| 1510.9(4) | 10(3) | 1836.0 | 325.0 | 1737.9(5) | 8(3) | | |
| 1516.5(4) | 9(3) | 1779.4 | 263.0 | 1742.0(3) | 15(3) | 1822.7 | 80.8 |
| 1518.7(5) ^d | 5(2) | | | 1749.3(2) | 30(10) | 1912.5 | 163.3 |
| 1523.2(4) | 14(4) | 1912.5 | 389.6 ^c | 1765.2(6) ^d | 4(2) | | |
| 1526.5(4) | 10(3) | | | 1771.3(6) ^d | < 2 | 2011.9 | 240.5 |
| 1528.4(2) | 57(10) | 1791.4 | 263.0 ^c | 1777.7(4) | 14(4) | 1858.3 | 80.8 |
| 1533.3(5) | 8(3) | 1858.3 | 325.0 | 1792.2(6) ^d | 5(2) | 1939.8 | 147.4 |
| 1537.2(2) | 80(15) | 1791.4 | 254.2 ^c | 1798.1(4) | 16(4) | 2011.9 | 213.8 ^c |
| 1549.0(5) | 9(3) | 1762.2 | 213.8 | 1809.8(6) ^d | 5(2) | 2024.2 | 213.8 |
| 1553.8(5) ^d | 6(3) | 2121.1 | 571.8 | 1824.5(7) ^d | 3(2) | 1824.9 | 0 |
| 1556.4(4) | 12(4) | | | 1833.1(5) | 8(3) | | |
| 1559.7(4) | 15(4) | 1822.7 | 263.0 | 1859.9(4) | 9(2) | 1939.8 | 80.8 |
| 1561.5(4) | 10(4) | 1824.9 | 263.0 | 1913.8(8) ^d | 2(1) | | |
| 1566.1(5) ^d | 6(3) | 1779.4 | 213.8 | 1924.4(8) ^d | 2(1) | | |
| 1570.7(2) | 65(8) | 1824.9 | 254.2 ^c | 1935.3(5) | 8(2) | | |
| 1572.6(4) | 13(4) | 1791.4 | 218.6 | 1949.8(6) | 4(2) | | |
| 1577.7(2) | 100(20) | 1791.4 | 213.8 ^c | 1978.4(7) ^d | 2(1) | | |
| 1583.6(2) | 55(9) | 2121.1 | 537.5 ^c | 2012.5(8) | 2(1) | 2011.9 | 0 |
| 1595.3(3) | 25(6) | 1858.3 | 263.0 ^c | 2023.7(6) | 7(2) | 2024.2 | 0 |

^a γ -ray intensities have been normalized to a value of 1000 for the 254.2-keV transition. There are 5.0(4) 254.2-keV γ rays per 100 decays.

^b Obtained from coincidence spectra.

^c The transition has been found to be in coincidence with one or more transitions exciting an initial level or deexciting a final level.

^d Only tentatively assigned to ¹⁵³Dy decay.

γ ray of any intensity and the resulting coincidence spectra were obtained. In the case of experiment (1) 196 gates were set, 156 of which yielded positive coincidence information. In experiment (2) 60 gates were set; some of these transitions were the same as those gated in experiment (1).

The results of the $\gamma\gamma$ coincidence experiment are indicated in Table I and Fig. 4. In Table I the levels which are coupled by a particular transition are identified by footnote c if that transition has

been found to be in coincidence with one or more transitions assigned as exciting the initial level or deexciting the final level. Similarly, in Fig. 4 circles are used to identify coincidence relationships.

The coincidence data of Ref. 5 are generally in agreement with the results shown in Table I but are much more limited in scope. Some significant discrepancies are these: In the 80.8-keV gate they do not report a 1050-keV γ ray which in our

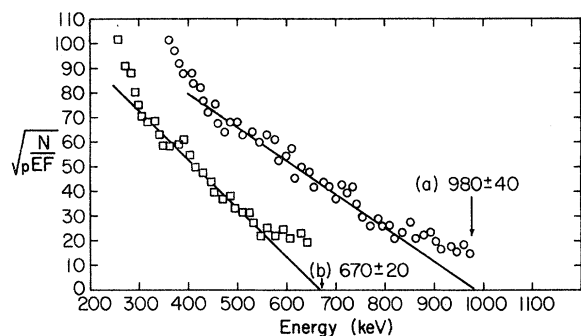


FIG. 2. Kurie plots for the β^+ decay of ^{153}Dy . The data are derived from β^+ coincidences with (a) 99.7-keV and (b) 274.5-keV γ rays. Lines only serve as a guide. End points were determined by a least-squares fit.

data is much more intense than the five γ rays they list above 1 MeV. Also, in the 99.7-keV gate they did not observe a strong 1375-keV transition and in the 274.5-keV gate they do not report the 235.4-keV transition.

A $\gamma\beta^+$ coincidence experiment was carried out to determine the Q value for ^{153}Dy decay. The γ -ray

detector was detector A and the β^+ detector was a cylindrical NE102 scintillator, 5 cm diam and 3.8 cm long. A total of 1.6×10^7 events was recorded. In five γ -ray gates β^+ spectra were obtained with sufficient intensity to analyze as Kurie plots. The data were corrected for summing with annihilation radiation. End-point energies were determined by a least-squares fit of the most linear portion of the Kurie plot. Typical Kurie plots are shown in Fig. 2.

The Q value deduced from the β^+ end-point energies in these spectra was 2250 ± 50 keV, in good agreement with the predicted value of 2220 keV by Wapstra and Gove,⁹ but significantly lower than the value 2350 keV listed in the tables of Garvey *et al.*¹⁰ and very much less than the old value of 2960 keV assumed by Harmatz and Handley.⁴

C. Conversion-electron spectra

A thin source of ^{153}Dy was made by evaporation of a few drops of a carrier-free ^{153}Dy solution on Al foil. The solution was prepared by taking up an ion-exchange-separated Dy fraction in CCl_4 . Con-

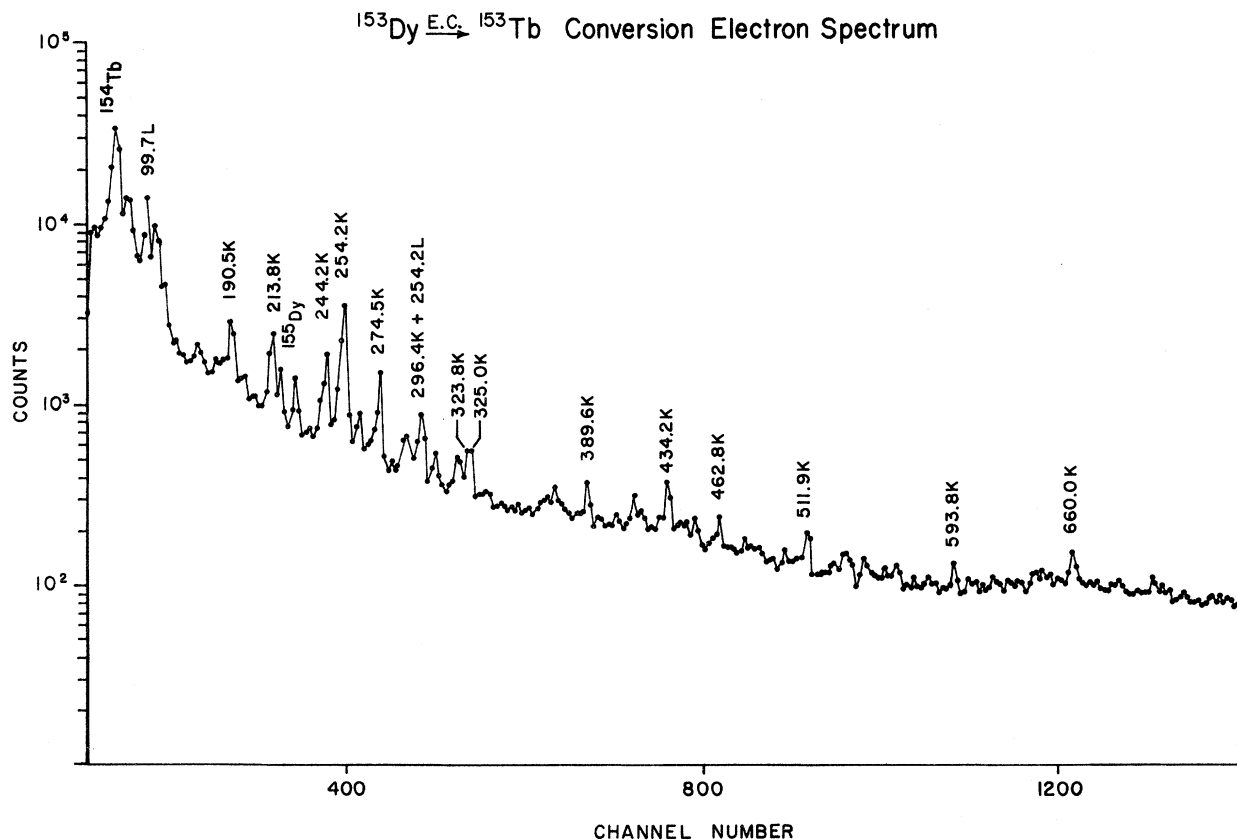


FIG. 3. Conversion-electron spectrum from the decay of 6.3-h ^{153}Dy . Peaks are labeled by transition energy. Only the more intense peaks are labeled to indicate the energy scale.

TABLE II. Intensities of K -conversion electrons, conversion coefficients, and multiplicities of transitions in 6.3-h ^{153}Dy decay.

| Transition energy (keV) | This work | I_K^a | | Exp. ^c | α_K | | This work | Multipolarity ^e | |
|-------------------------|--------------|---------------|---------------------|-------------------|--------------------|-------------|-----------|----------------------------|--------------|
| | | Ref. 4 | Ref. 5 ^b | | Theo. ^d | Ref. 4 | | Ref. 5 | |
| 70.8 | | 56 | | 6(1) | $M1: 5.4$ | $M1$ | | $M1$ | $M1$ |
| 71.1 | | 18 | | 5(2) | $M1: 5.4$ | $M1$ | | | |
| 80.8 | | 3740 | | 2.7(4) | $M1: 3.6$ | $M1+E2$ | | $M1/E2=80$ | $M1+E2$ |
| 82.5 | | 3150 | | 32(5) | $M2: 33$ | $M2$ | | $M2$ | $M2$ |
| 93.1 | | 245 | | 2.1(3) | $M1: 2.4$ | $M1$ | | $M1/E2=30$ | $M1+E2$ |
| 99.7 | | 1960 | | 1.6(2) | $M1: 1.9$ | $M1(E2)$ | | $M1/E2=39$ | $M1+E2$ |
| 127.2 | | 3.9 | | 1.0(2)-1 | $E1: 1.4-1$ | $E1$ | | | $E1$ |
| 128.2 | | 38 | | 1.1(2) | $M1: 9.4-1$ | $M1$ | | $M1/E2=3$ | $M1+E2$ |
| 133.0 ^f | | 6 | | 1.7(3)-1 | $E1: 1.3-1$ | $E1$ | | | |
| 147.4 | | 213 | | 5.1(8)-1 | $M1: 6.3-1$ | $M1+E2$ | | $M1/E2=5$ | $M1$ |
| 149.0 | | 60 | | 6.3(10)-1 | $M1: 6.3-1$ | $M1$ | | $M1$ | $M1$ |
| 173.3 | 19(3) | 18.9 | | 4.5(7)-1 | $M1: 4.0-1$ | $M1$ | | | ($M1$) |
| 182.4 | 14(3) | 18 | | 4.4(9)-1 | $M1: 3.6-1$ | $M1$ | | | $M1$ |
| 185.6 ^g | 8(2) | 12 | | 3.3(8)-1 | $M1: 3.4-1$ | ($M1$) | | | |
| 190.5 | 34(3) | 35 | | 3.1(3)-1 | $M1: 3.1-1$ | $M1$ | | $M1/E2 \approx 10$ | $M1$ |
| 193.8 | 2.4(10) | 2.4 | | 5(2)-2 | $E1: 4.3-2$ | $E1$ | | | ($E1$) |
| 204.3 | 6.5(16) | 10 | | 1.9(5)-1 | $M1: 2.5-1$ | $M1(E2)$ | | | $M1$ |
| 213.8 | 42(3) | ≈ 40 | | 3.2(2)-2 | $E1: 3.2-2$ | $E1$ | | $M1+E2$ | $E1$ |
| 218.6 | 36(3) | 34 | | 2.1(2)-1 | $M1: 2.2-1$ | $M1$ | | | $M1$ |
| 240.6 | 8(2) | 11 | 6.9 | 1.9(5)-1 | $M1: 1.7-1$ | $M1$ | | $M1$ | $M1$ |
| 242.0 | 3.1(12) | 2.2 | | 1.9(7)-1 | $M1: 1.6-1$ | $M1$ | | | $M1$ |
| 244.2 | 60(6) | 71 | | 1.2(1)-1 | $M1: 1.6-1$ | $M1+E2$ | | ($M1$) | $\equiv M1$ |
| 247.4 | 1.6(10) | 2.5 | | 3(2)-2 | $E1: 2.3-2$ | $E1$ | | | $E1$ |
| 254.2 | $\equiv 140$ | $\equiv 140$ | | 1.4(1)-1 | $M1: 1.4-1$ | $\equiv M1$ | | $M1$ | $M1$ |
| 262.4 | 14(2) | 14 | | 1.3(2)-1 | $M1: 1.3-1$ | $M1$ | | | $M1+E2$ |
| 274.5 | 49(4) | 62 | | 5.9(5)-2 | $E2: 6.2-2$ | $E2$ | | $M1$ | $M1+E2$ |
| 289.0 | 2.5(11) | ≈ 5.2 | 3.1 | 9(4)-2 | $M1: 1.0-1$ | ($M1$) | | | $M1$ |
| 290.8 | 6.0(15) | 8.5 | 5.11 | 9(2)-2 | $M1: 1.0-1$ | $M1$ | | | $M1+E2$ |
| 296.4 ^g | <7 | ≈ 3.9 | 2.62 | <4-2 | $E2: 5.1-2$ | ($E1$) | | | |
| 302.6 | 1.9(9) | 2.0 | | 8(4)-2 | $M1: 8.9-2$ | ($M1$) | | | |
| 323.8 | 13(2) | 12 | 7.88 | 9(1)-2 | $M1: 7.5-2$ | $M1$ | | | $M1+E2$ |
| 325.0 | 6(1) | <5.3 | 3.5 | 8(1)-2 | $M1: 7.5-2$ | $M1$ | | | $E2$ |
| 334.5 | 2.2(8) | 2.2 | 2.2 | 8(3)-2 | $M1: 7.3-2$ | $M1$ | | | $M1$ |
| 363.9 | 2.6(9) | 3.1 | | 7(2)-2 | $M1: 5.3-2$ | $M1$ | | | |
| 371.6 | 3.2(9) | 5.3 | | 3(1)-2 | $E2: 2.6-2$ | ($E2$) | | | |
| 376.2 ^g | 1.4(7) | 1.4 | 1.89 | 4(2)-2 | $M1: 5.0-2$ | ($M1$) | | | |
| 383.6 | 1.1(5) | 1.1 | | 4(2)-2 | $M1: 4.8-2$ | ($M1$) | | | |
| 389.6 | 7.2(11) | 10.8 | 5.25 | 4.4(7)-2 | $M1: 4.6-2$ | $M1$ | | | $M1+E2$ |
| 405.9 | 1.3(6) | 3.5 | 1.5 | 2.6(11)-2 | $E2: 2.0-2$ | ($E2$) | | | $M1+E2$ |
| 415.8 | 4.5(9) | 6.7 | 3.47 | 3.5(7)-2 | $M1: 4.0-2$ | $M1(E2)$ | | | $M1$ |
| 420.1 | 2.7(10) | 3.2 | 1.65 | 4.1(15)-2 | $M1: 3.8-2$ | ($M1$) | | | $M1+E2$ |
| 429.6 | 1.8(6) | 2.0 | 0.90 | 5.4(18)-2 | $M1: 3.6-2$ | ($M1$) | | | $M1$ |
| 434.2 | 9.4(29) | 13 | 5.85 | 5.9(18)-2 | $M1: 3.5-2$ | ($M1$) | | | ($M1$) |
| 441.6 | 1.2(5) | 1.5 | 0.92 | 2.9(12)-2 | $M1: 3.3-2$ | ($M1$) | | | $M1+E2$ |
| 444.7 | 2.1(6) | 2.6 | 1.58 | 1.4(4)-2 | $E2: 1.7-2$ | $E2$ | | | $M1+E2$ |
| 448.8 | 2.1(6) | 3.2 | 2.03 | 1.6(5)-2 | $E2: 1.7-2$ | $E2$ | | | $M1+E2$ |
| 451.6 | 1.7(6) | 2.9 | | 3.0(10)-2 | $M1: 3.0-2$ | $M1$ | | | |
| 462.6 | 3.3(8) | 6.4 | 3.47 | 3.5(8)-2 | $M1: 2.9-2$ | $M1$ | | | |
| 471.4 | 1.0(4) | 1.1 | 0.48 | 6.4(26)-3 | $E1: 4.4-3$ | $E1$ | | | ($E1$) |
| 500.0 | 1.4(7) | 1.4 | 0.73 | 4.1(20)-2 | $M1: 2.4-2$ | ($M1$) | | | $M1$ |
| 511.9 | 4.5(10) | 5.0 | | 16(3)-3 | $M1: 2.3-2$ | $M1+E2$ | | | |
| 513.1 | <0.3 | ≈ 1.8 | 3.33 | <4-3 | $E1: 4.2-3$ | ($E1$) | | | |
| 527.3 | 0.4(1) | ≈ 0.6 | 0.39 | 6.2(15)-3 | $E1: 4.2-3$ | ($E1$) | | | $E1$ |
| 535.8 | 0.6(2) | 1.6 | 0.81 | 2.8(9)-2 | $M1: 2.0-2$ | $M1$ | | | $M1+(E2+E0)$ |
| 537.5 | 0.7(3) | 0.91 | 0.45 | 4.4(19)-3 | $E1: 4.1-3$ | $E1$ | | | $E1$ |
| 544.8 | 1.5(5) | 2.1 | 1.11 | 2.5(8)-2 | $M1: 1.9-2$ | $M1$ | | | |
| 562.3 | 1.7(5) | 2.2 | 0.91 | 2.4(7)-2 | $M1: 1.8-2$ | $M1$ | | | $M1+E2$ |

TABLE II. (Continued)

| Transition energy (keV) | I_K^a | | α_K | | | Multipolarity ^e | | |
|-------------------------|-----------|--------|---------------------|-------------------|--------------------|----------------------------|--------|-----------|
| | This work | Ref. 4 | Ref. 5 ^b | Exp. ^c | Theo. ^d | This work | Ref. 4 | Ref. 5 |
| 571.8 | 0.6(2) | 0.6 | 0.22 | 1.5(5)–2 | $M1 : 1.7 - 2$ | $M1(E2)$ | | $E2 + M1$ |
| 579.3 | 0.6(2) | 0.6 | 0.34 | 1.1(3)–2 | $M1 : 1.6 - 2$ | $M1 + E2$ | | $M1$ |
| 593.8 | 1.8(4) | 3.5 | 2.04 | 1.3(3)–2 | $M1 : 1.5 - 2$ | $M1$ | | $M1$ |
| 614.3 | 0.8(3) | | | 1.3(5)–2 | $M1 : 1.4 - 2$ | ($M1$) | | |
| 644.5 | 0.6(3) | ≈0.6 | 0.66 | 1.6(8)–2 | $M1 : 1.3 - 2$ | ($M1$) | | ($M1$) |
| 652.7 | <0.2 | | 0.29 | <8–3 | $E2 : 6.1 - 3$ | ($E1, E2$) | | $M1$ |
| 660.0 | 3.4(7) | 3.1 | 2.02 | 2.5(5)–2 | $M1 : 1.2 - 2$ | $M1 + (E2 + E0)$ | | ($M1$) |
| 704.0 | 0.4(1)} | 0.4 | 0.36 | 1.3(3)–2 | $M1 : 1.0 - 2$ | $M1$ | | $M1$ |
| 705.8 | 0.6(2)† | | | | | | | |

^a Intensities in this work normalized to 140 for the 254.2-keV transition. Relative intensities reported in Refs. 4 and 5 have been multiplied by the factor 1.40.

^b Below 289 keV (except at 240.6 keV) I_K values are the same as those in Ref. 4. Many other electron lines, not observed in this work, are reported in Ref. 5.

^c Experimental α_K values are from this work only; for transitions below 173 keV, I_K values from Ref. 4 have been used. Read an entry such as 6.3(10)–1 as $(6.3 \pm 1.0) \times 10^{-1}$.

^d Interpolated from Ref. 12.

^e For the purposes of this table and the discussion in the text, the designation $M1$ (or $E2$) is not intended to exclude the possibility of a small admixture of $E2$ (or $M1$) in the transition; when the experimental α_K value is intermediate between $M1$ and $E2$, the assigned multipolarity is shown as mixed.

^f Assumed to be the same transition as that reported in Ref. 4 at 135.35 keV.

^g May be a doublet.

version-electron spectra were obtained with a cooled Si(Li) electron spectrometer.¹¹ Typical resolution (FWHM) was 2.5 keV at 1000 keV. A spectrum is shown in Fig. 3.

Intensities of K -conversion lines determined in this work are listed in Table II. Normalization of the electron and γ -ray intensity scales has been made at 254 keV. This strong transition is known from its L_V/L_{III} subshell ratio to be a pure $M1$ transition.⁴ The two scales were chosen so that the I_K values in column 2 of Table II, when divided by the I_γ values of Table I, result in the α_K values shown in column 5. Theoretical α_K values are interpolated from Hager and Seltzer.¹²

Where the data overlap, the multiplicities assigned to transitions from conversion coefficients measured in this work generally agree with the assignments of Harmatz and Handley.⁴ A notable exception is the 213.8-keV transition which is identified as $M1 + E2$ in Ref. 4; our data clearly indicate that the transition is $E1$. In the previous work this transition was part of an unresolved doublet; no such ambiguity is observed in the present result.

The conversion-electron intensity scale of Zuber *et al.*⁵ is said to be normalized to the γ -ray intensity scale on the assumption that the 244.2-keV transition is pure $M1$. Harmatz and Handley⁴ find this line to be part of a partially resolved mul-

tiplet and only tentatively assign it as $M1$. Our data indicate that this transition may have a considerable $E2$ admixture. The reported normalization is somewhat puzzling since Zuber *et al.*⁵ do not report their own electron intensities below 289 keV except for the 240.6-keV transition; in this energy range all other entries as well as multipolarity assignments are from Harmatz and Handley. In general, the agreement between our data and those of Zuber *et al.* is satisfactory. While no experimental uncertainties are reported in the latter work, the intensities listed in Table II reflect the precision with which experimental data were reported.

Included in Table II also are conversion-electron intensities as reported by Harmatz and Handley⁴ and Zuber *et al.*⁵ The intensities of Refs. 4 and 5 have been normalized to the scale we use. For transition energies below 173 keV, the I_K data of Ref. 4 are superior to our data and have been used together with our I_γ values to obtain α_K values. In both Refs. 4 and 5 additional K lines, not observed in this work, were reported; in some cases γ rays corresponding to these transitions were found in our spectra. However, these transitions have not been included in Table II since experimental uncertainties in intensities are not explicitly stated in Refs. 4 and 5 and the assignment of multiplicities would be doubtful.

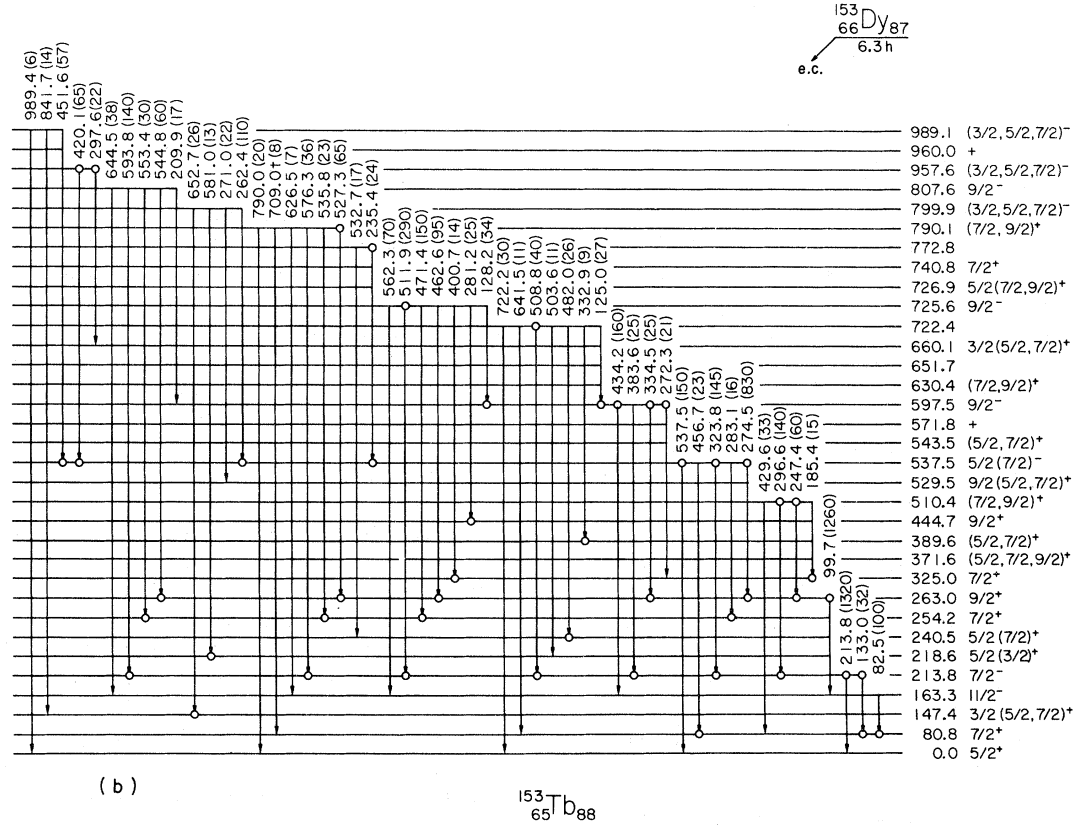
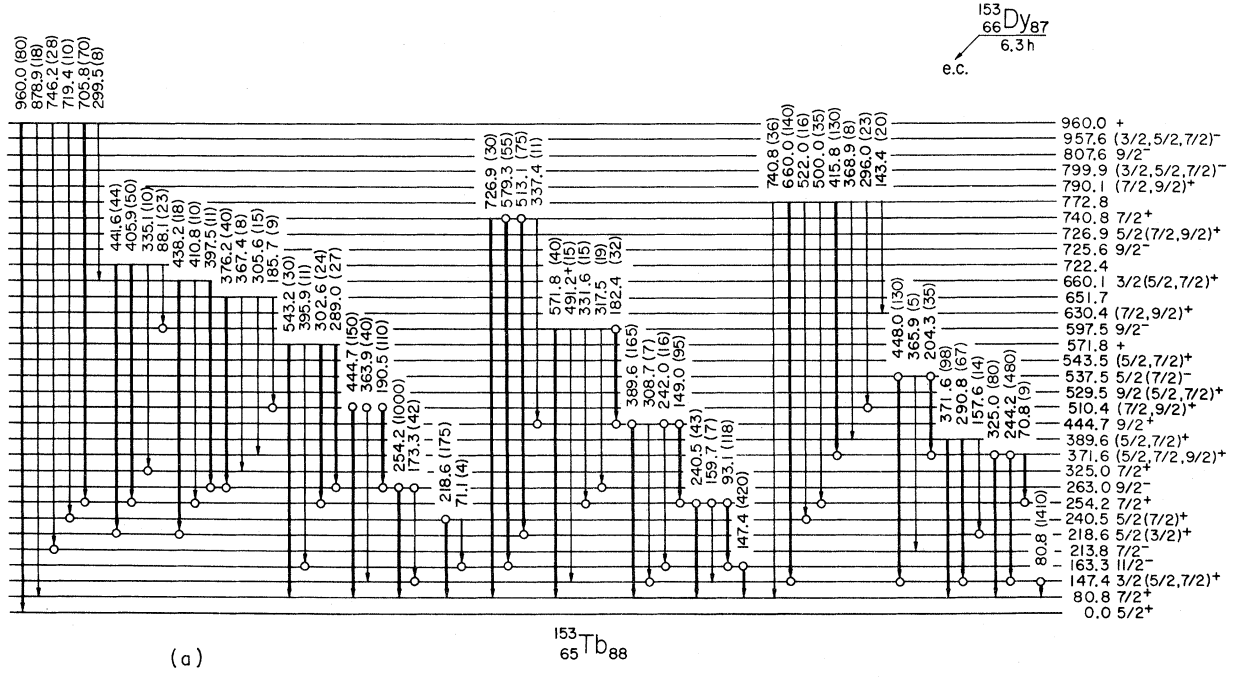


FIG. 4. Decay scheme for ^{153}Dy decay to levels in ^{153}Tb . Energies are in keV. In (a) the heavy lines indicate principal deexcitation paths. Circles identify coincidence relationships. A cross after a transition energy indicates that the transition has been placed more than once. Spin-parity assignments are based on transition multipolarities and not on $\log ft$ values.

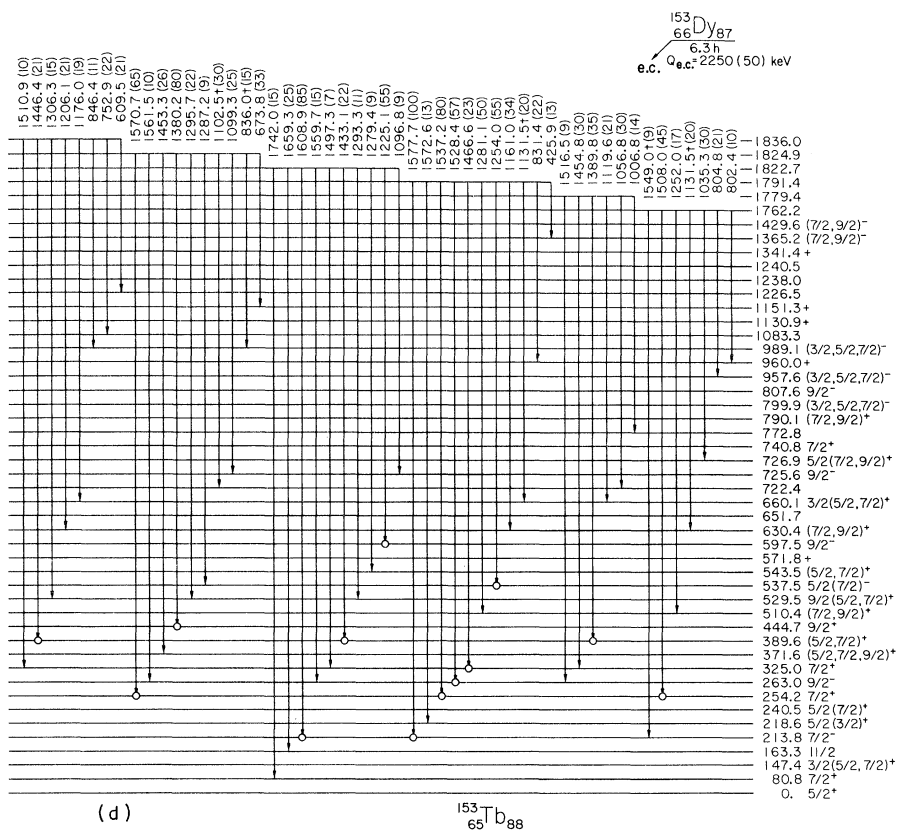
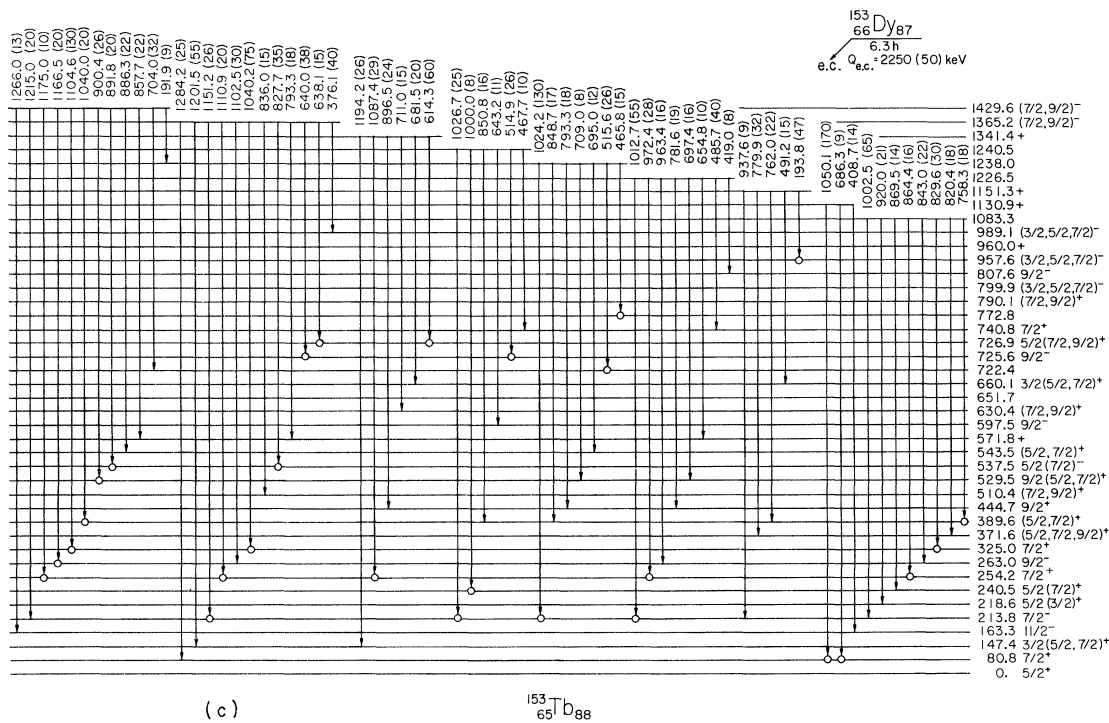


FIG. 4. (Continued)

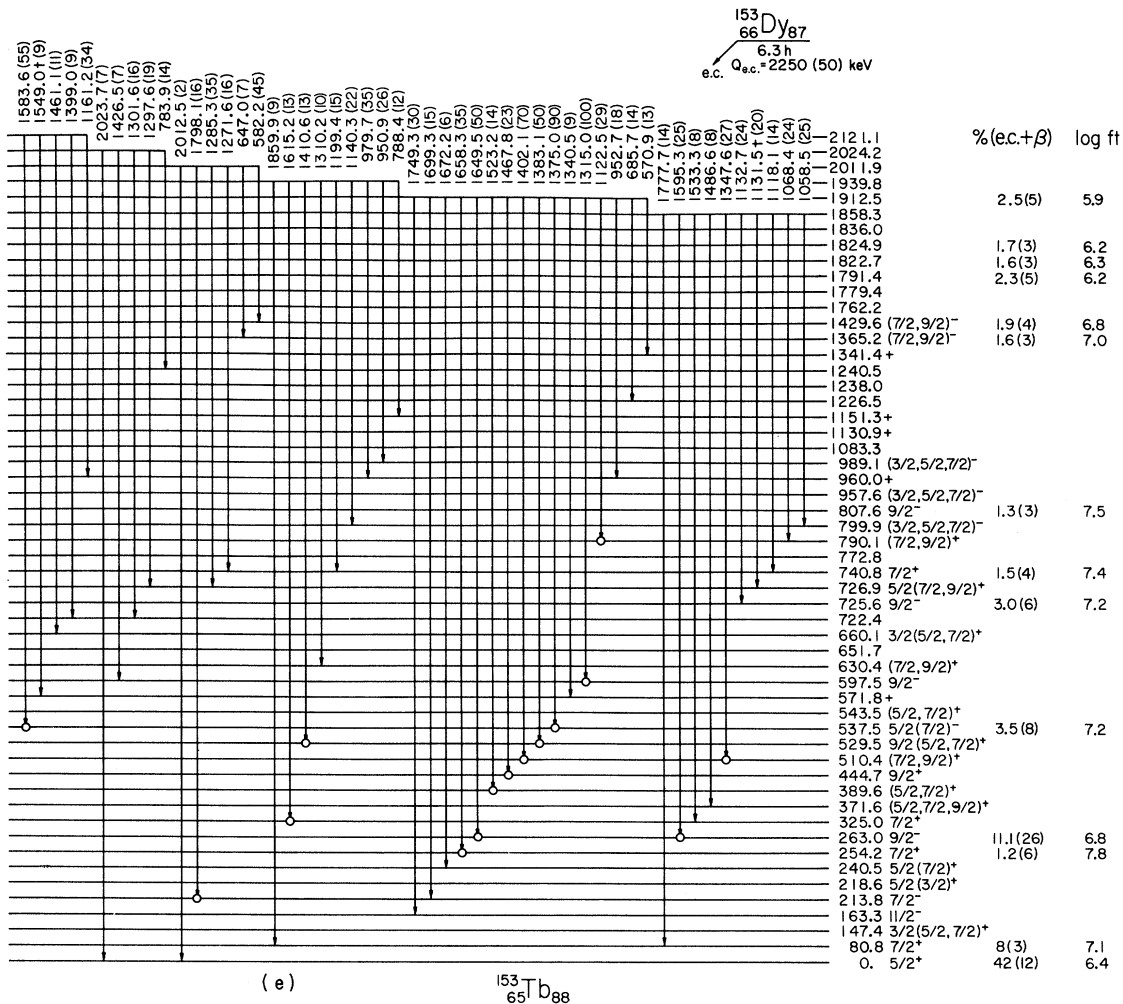


FIG. 4. (Continued)

III. LEVEL SCHEME OF ^{153}Tb

A. Level assignments

Transitions observed in ^{153}Dy decay have led to the determination of 54 levels as shown in Figs. 4(a)–4(e). Of the 400 γ rays in Table I, 193 have been placed by coincidence data and 126 by energy sums; 81 have not been placed. In all but one of these levels, coincidence data were used to establish the existence of a level. For low-lying levels (<1 MeV), an average of seven coincidence-assigned transitions was associated with each level. Circles are used on the level scheme to identify such transitions.

The first few excited states in ^{153}Tb at 80.8, 147.4, and 254.2 keV are well known from previous work,^{4,5} and the present data confirm that these levels deexcite directly to the ground state. In both this work and in Ref. 5 the ground-state de-

cay of levels at 213.8 and 218.6 keV has been observed. The $\frac{11}{2}^-$ isomeric state, whose half-life is 173 μsec ,¹³ deexcites by an 82.5-keV transition to the 80.8-keV state⁴; the energy of the isomeric state is thus 163.3 keV. Starting with this basic skeleton for the lowest-lying states, we were able to generate the level scheme shown in Fig. 4.

Generally the level of confidence in identifying the energy levels is very high because of the interlocking and multiple coincidence information. For a few levels, however, only one or two coincident transitions were observed (e.g., the levels at 651.7, 772.8, and 1151.3 keV), or in one case none (2024.2 keV), and the existence of these levels is less certain.

Many of the lower-lying levels in Figs. 4(a) and 4(b) are found also in the level scheme of Zuber *et al.*⁵ However, 11 levels in their scheme at 452.0, 802.1, 832.6, 1087.1, 1104.6, 1192.0,

1332.2, 1512.3, 1516.5, 1570.2, and 1577.3 keV are not supported by our coincidence data. Levels which we have established but which are not reported in Ref. 5 are at 371.6, 543.5, 651.7, 722.4, 772.8, and 1083.3 keV and all higher-lying levels except those at 1791.4, 1822.7, and 1912.5 keV.

The lower-lying levels proposed by Harmatz and Handley⁴ are also generally confirmed by this work. The largest discrepancy concerns the level they propose at 323.8 keV. The 213.8- and 323.8-keV transitions are in coincidence. The intensity relationship between these two requires that the 323.8-keV transition precede the 213.8-keV transition and not the reverse as indicated in Ref. 4. In addition, levels they report at 452.2, 674.7, 692.2, 766.0, 943.6, 967.4 keV are not supported by our coincidence data.

B. Spin and parity assignments

Atomic-beam measurements have shown that the spins of ¹⁵³Tb (Ref. 14) and ¹⁵³Dy (Ref. 15) are $\frac{5}{2}$ and $\frac{7}{2}$, respectively, and other evidence⁴ indicates their parities are positive and negative, respectively. The remaining spin and parity assignments are based on the transition multipolarities indicated in Table II.

C. Excitation-deexcitation properties of levels

In a level scheme as complex as that of ¹⁵³Tb, we find it important to search for possible systematic groupings of levels which would tend to simplify their interpretation. We have found it illuminating to group the positive-parity levels according to their major deexcitation paths. This is indicated in Fig. 4(a). The darkened transitions are those that carry off most of the intensity of a particular level. Groups of levels have been found that decay principally to a low-lying positive-parity state or to a level which in turn decays to that low-lying state. Groups are identified by the low-lying level to which they decay. These are at 80.8, 147.4, and 254.2 keV. We would like to point out that the systematics of states^{16,17} in ¹⁵¹Eu and ¹⁴⁹Pm suggest that the positive-parity 147.4-keV level spin should be $\frac{3}{2}$, although $\frac{5}{2}$ and $\frac{7}{2}$ are not excluded by the present data.

The segregation of levels into groups which populate negative-parity levels does not establish clear patterns similar to those of the positive-parity levels. Almost all negative-parity levels decay primarily to the 213.8-keV $\frac{7}{2}^-$ level and to the 263.0-keV $\frac{9}{2}^-$ level. There are three positive-parity levels (510.4, 790.1, and 1151.3 keV), and five levels of unknown parity which decay predominantly to the 213.8-keV level and/or the 263.0-keV level and thus have been included with the negative-

parity levels in Fig. 4(b).

In Figs. 4(c), 4(d), and 4(e) are indicated the de-exciting transitions of the 21 levels lying between 1000 and 2121 keV. Electron capture most strongly populates levels at 1365.2, 1429.6, 1791.4, 1822.7, 1824.9, and 1912.5 keV. Their deexcitation is primarily to levels below 600 keV. $\log ft$ to the 1912.5-keV level implies an allowed β decay, limiting it to spin values of $\frac{5}{2}$, $\frac{7}{2}$, or $\frac{9}{2}$ with negative parity. The other levels listed have $\log ft$ values consistent with allowed or first-forbidden β transitions, limiting their spins to $\frac{5}{2}$, $\frac{7}{2}$, or $\frac{9}{2}$ with either parity possible. Spins and parities are not shown in Figs. 4(c), 4(d), and 4(e) if β -decay systematics are the only basis available for making assignments.

IV. DISCUSSION

A. Qualitative aspects of low-lying positive-parity states

The odd- Z , $N = 88$ nuclei ¹⁵¹Eu (Ref. 16) and ¹⁴⁹Pm (Ref. 17) have been qualitatively interpreted in the context of the weak-coupling model. In the case of ¹⁵³Tb, Harmatz and Handley⁴ and Zuber *et al.*⁵ characterize the $\frac{5}{2}^+$ ground state, the $\frac{7}{2}^+$ 80.8-keV state, and the $\frac{11}{2}^-$ 163.3-keV state as the $d_{5/2}$, $g_{7/2}$, and $h_{11/2}$ shell-model states, respectively. The remaining low-lying positive-parity states might then be composed of one- and two-phonon quadrupole vibrations coupled to the $d_{5/2}$ and $g_{7/2}$ states. One would expect predominantly $E2$ transitions from two-phonon to one-phonon states, and from one-phonon states to the zero-phonon ground and 80.8-keV states. Transitions from two-phonon states to zero-phonon states should be hindered. The experimental evidence is in disagreement with such an interpretation. The low-lying positive-parity levels at 218.6, 240.5, 254.2, 325.0, and 389.6 keV have ground-state transitions that appear to be $M1$. Many of the higher-lying states, presumably of two-phonon character, have strong transitions to either the ground or 80.8-keV states. While mixing of the $d_{5/2}$ and $g_{7/2}$ states could enhance the $M1$ transition probabilities, it would also cause spreading of the weak-coupling multiplets and lead to a reduced level density. A more sophisticated method applicable to the case of stronger coupling may be necessary.¹⁸ The recent proton-transfer studies⁶ are also inconsistent with a simple shell-model description.

An alternative to the weak-coupling description would be to describe the odd-proton in ¹⁵³Tb in terms of Nilsson states. The bandlike structure of the level groups in Fig. 4(a) also suggests such an interpretation. Thus the $\frac{5}{2}^+$ ground state and the $\frac{7}{2}^+$ 80.8-keV state might be members of a rotational

TABLE III. Ratio of ft values for populating $\frac{5}{2}^+$ and $\frac{7}{2}^+$ final states in transitional and deformed nuclei from a parent $\frac{7}{2}^-$ state.

| Daughter nucleus | N | $ft(\frac{5}{2}^+)$ | |
|-------------------|-----|---------------------|-----------|
| | | $ft(\frac{7}{2}^+)$ | Reference |
| Spherical | | 2.4 | 20 |
| ^{149}Eu | 86 | 2.5 | 21 |
| ^{149}Pm | 88 | >10 | 17 |
| ^{151}Eu | 88 | >15 | 16 |
| ^{153}Tb | 88 | 0.2 ± 0.1 | This work |
| ^{153}Eu | 90 | <0.1 | 22 |
| Rotational limit | | 0.30 | 19 |

band. If this were the case, the ratio of ft values for β transitions to the $\frac{5}{2}^+$ and $\frac{7}{2}^+$ states would be given by squares of the appropriate Clebsch-Gordan coefficients,¹⁹ that is, the ratio R would be

$$R = \frac{\langle \frac{7}{2}^- \frac{7}{2}^- 1-1 | \frac{7}{2}^- \frac{5}{2}^+ \rangle^2}{\langle \frac{7}{2}^- \frac{7}{2}^- 1-1 | \frac{7}{2}^- \frac{7}{2}^+ \rangle^2} = 0.30.$$

On the other hand, in spherical nuclei, if the parent state is $f_{7/2}$ and the daughter states are $g_{7/2}$ and $d_{5/2}$, R is 2.4.²⁰ For ^{153}Tb R is 0.2 ± 0.1 ; experimental values of R for several transitional and deformed nuclei^{16,17,21,22} are listed in Table III. Although neither model used to predict R values is expected to apply very well to a transitional nucleus like ^{153}Tb , the observed trend suggests that a quasirotational interpretation may be appropriate.

Low-lying positive-parity Nilsson states identified in more deformed Tb nuclei are $\frac{3}{2}^+[411]$, $\frac{5}{2}^+[413]$, $\frac{5}{2}^+[402]$, and $\frac{7}{2}^+[404]$. These have been observed in ($^3\text{He}, d$) and (α, t) reaction studies,³ in radioactive decay,^{23,24} and in ($\alpha, xn\gamma$) studies.²⁵ At the small deformation expected for ^{153}Tb , the Coriolis force is expected to induce considerable mixing of these states. Thus in the present dis-

cussion, references to specific Nilsson states and members of their rotational bands are made with the implicit understanding that other components are invariably present.

In the region of 65 protons the ground state and $\frac{7}{2}^+$ 80.8-keV state could arise from either the $\frac{5}{2}^+[413]$ or $\frac{5}{2}^+[402]$ Nilsson orbitals. The most likely candidate for the other $\frac{5}{2}^+$ bandhead is the state at 218.6 keV. Two pairs of $\frac{7}{2}^+$ and $\frac{9}{2}^+$ states have similar deexcitation patterns. These are the pairs at 254.2 and 444.7 keV and at 325.0 and 529.5 keV. One pair could be the members of a rotational band with its bandhead at 218.6 keV, while the other pair could be the bandhead and first rotational excitation from the $\frac{7}{2}^+[404]$ Nilsson orbital. The state at 371.6 keV, which decays primarily into the ground-state band and whose spin-parity is $(\frac{5}{2}, \frac{7}{2}, \frac{9}{2})^+$, may be the $\frac{9}{2}^+$ member of the ground-state band, although the energy is somewhat higher than might be expected. On the other hand, the experimental energy seems rather low for this state to result from a vibrational excitation and we very tentatively assign the 371.6-keV state as the $\frac{9}{2}^+$ member of the ground-state band. The most likely state for the $\frac{3}{2}^+[411]$ bandhead is at 147.4 keV. From Fig. 4(a), one can see that a cascade of transitions relates the 147.4-keV level to levels at 240.5, 389.6, and 571.8 keV. We suggest that these levels are the $\frac{5}{2}^+$, $\frac{7}{2}^+$, and $\frac{9}{2}^+$ members of the $\frac{3}{2}^+[411]$ rotational band. A similar interpretation of these four levels has been made by Zuber *et al.*⁵

To choose between $\frac{5}{2}^+[413]$ and $\frac{5}{2}^+[402]$ as the better representation of the ground state, we have examined the decay characteristics of the $\frac{7}{2}^+$ level at 325.0 keV. This level deexcites to the ground state, the $\frac{7}{2}^+$ 80.8-keV state, and the $\frac{7}{2}^+$ 254.2-keV state. There are two possible assignments for the ground and 80.8-keV states, and two possible assignments each for the $\frac{7}{2}^+$ states at 254.2 and 325.0 keV. The various possibilities are shown in Table IV. Relative $B(M1)$ values [normalized

TABLE IV. Relative $B(M1)$ values for various assignments of experimental levels as Nilsson states.

| Ground state | 254.2 keV | 325.0 keV | 325.0 \rightarrow 254.2 | $B(M1)$ values | |
|----------------------|-------------------------------------|-------------------------------------|---------------------------|-----------------------|---------------------------------------|
| | | | | 325.0 \rightarrow 0 | 325.0 \rightarrow 80.8 ^a |
| $\frac{5}{2}^+[413]$ | $\frac{7}{2}^+[404]$ | $\frac{7}{2}^+, \frac{5}{2}^+[402]$ | 1.0 | 3.4 | 6.3 |
| $\frac{5}{2}^+[413]$ | $\frac{7}{2}^+, \frac{5}{2}^+[402]$ | $\frac{7}{2}^+[404]$ | 1.0 | 106 | 31 |
| $\frac{5}{2}^+[402]$ | $\frac{7}{2}^+[404]$ | $\frac{7}{2}^+, \frac{5}{2}^+[413]$ | 1.0 | 0.11 | 0.20 |
| $\frac{5}{2}^+[402]$ | $\frac{7}{2}^+, \frac{5}{2}^+[413]$ | $\frac{7}{2}^+[404]$ | 1.0 | 0.11 | 0.032 |
| Experimental value | | | 1.0 | 0.09 ± 0.02 | 0.6 ± 0.2^b |

^aIn each case the 80.8-keV state is taken to be the $\frac{7}{2}^+$ member of the ground-state band.

^bCorrected for the $E2$ component in the 244.2-keV transition.

to $B(M1, 325.0 \rightarrow 254.2)$ have been calculated from $M1$ matrix elements tabulated by Browne and Femenia.²⁶ We have assumed that the deformation β is 0.1, $g_R = Z/A$, and $g_S = 0.6g_S(\text{free}) = 3.35$. The calculated values are not sensitive to the choice of β between 0.1 and 0.2. The experimental data clearly favor the choice $\frac{5}{2}^+[402]$ for the ground state. The assignments $\frac{7}{2}^+[404]$ for the 254.2-keV state and $\frac{7}{2}^+, \frac{5}{2}^+[413]$ for the 325.0-keV state appear likely. The reaction studies of Straume *et al.*⁶ are consistent with a $\frac{5}{2}^+[402]$ description of the ground state but they favor a $\frac{7}{2}^+[404]$ interpretation of the 80.8-keV state.

The electron-capture decay²⁷ of ^{153}Tb predominantly (57%) populates a $\frac{3}{2}^+$ level in ^{153}Gd at 212 keV with a $\log ft$ value of 6.8. This state in ^{153}Gd has been assigned as the $\frac{3}{2}^+[402]$ Nilsson state.²⁸ If this is the case and the ground state of ^{153}Tb is $\frac{5}{2}^+[402]$, the $\log ft$ value is much too large; one would expect an allowed unhindered transition with $\log ft < 5$. As we show later, the ^{153}Tb ground state undoubtedly is mixed and contains other components such as $\frac{3}{2}^+[411]$, but the dominant amplitude is from $\frac{5}{2}^+[402]$. Bunker and Reich²⁹ have pointed out that low-lying $\frac{3}{2}^+$ states in Gd, Dy, and Er nuclei have a strongly mixed $\{[651], [402]\}$ character. This may help to explain the retarded electron-capture decay of ^{153}Tb .

In the rotational model, the cascade-to-cross-over branching ratios within a band in an odd- A nucleus provide information on the g factors in the band. The quantity $|(g_K - g_R)/Q_0|$, where Q_0 is the intrinsic quadrupole moment, is expected to be a constant for all the rotational states in an unperturbed band.³⁰ For ^{153}Tb this test can be applied only among the levels in the $\frac{3}{2}^+[411]$ band. The results are summarized in Table V for ^{153}Tb and more deformed Tb nuclei. To the extent that data

TABLE V. Values of the rotational parameter $|(g_K - g_R)/Q_0|$ for members of the $\frac{3}{2}^+[411]$ band in Tb nuclei.

| Initial spin | ^{153}Tb ^a | ^{155}Tb ^b | ^{157}Tb ^b | ^{159}Tb ^c |
|----------------|--------------------------------|--------------------------------|--------------------------------|--------------------------------|
| $\frac{7}{2}$ | 0.28 | 0.18 | 0.19 | 0.18 |
| $\frac{9}{2}$ | 0.31 | 0.19 | 0.20 | 0.17 |
| $\frac{11}{2}$ | | 0.19 | 0.20 | 0.19 |
| $\frac{13}{2}$ | | 0.19 | 0.21 | 0.18 |
| $\frac{15}{2}$ | | 0.20 | 0.22 | 0.20 |
| $\frac{17}{2}$ | | 0.21 | 0.20 | |
| $\frac{19}{2}$ | | 0.20 | 0.20 | |

^aThis work.

^bReference 25.

^cReference 23.

are available, ^{153}Tb satisfies the constancy test. The magnitude of the quantity is substantially larger for ^{153}Tb than for more deformed nuclei. This is as expected since Q_0 should be smaller for ^{153}Tb and the g factors should be approximately independent of deformation.

Low-lying positive-parity levels are thus characterized in a deformed basis as shown in Fig. 5. A quantitative description of these levels is presented in the next section.

B. Coriolis-coupled bands in ^{153}Tb

The Nilsson states shown in Fig. 5 are expected to be mixed by the Coriolis interaction. In this section we calculate the effect of the mixing on Nilsson energies and transition probabilities. The energy $E(I, K)$ of an unperturbed state is given by³¹

$$E(I, K) = E(K) + A[I(I+1) - 2K^2 + \langle \vec{j}^2 \rangle + (-)^{I+1/2}(I + \frac{1}{2})\alpha\delta_{K, 1/2}], \quad (1)$$

where $E(K)$ is the quasiparticle energy (discussed below), A is the rotational constant $\hbar^2/2\mathcal{I}$ (\mathcal{I} is the moment of inertia), \vec{j} is the angular momentum of the odd particle, and α is the decoupling parameter for a $K = \frac{1}{2}$ band. The energy $E(K)$ is defined by³²

$$E(K) = [(\epsilon_K - \lambda)^2 + \Delta^2]^{1/2} - \Delta, \quad (2)$$

where ϵ_K is the single-particle energy of a particular Nilsson state, λ is the energy of the Fermi surface, and Δ is the gap parameter.

The eigenvalues and eigenvectors of the mixed states are obtained by diagonalizing a matrix for each spin value in which the diagonal elements are given by Eq. (1) and the off-diagonal elements by $-A'(K, K+1)[(I-K)(I+K+1)]^{1/2}\langle K+1 | j_x | K \rangle$. (3)

Here A' is $AF(K, K+1)$; the factor $F(K, K+1)$ includes the BCS occupation term ($U_K U_{K+1} + V_K V_{K+1}$) and a term which adjusts (generally attenuates)

| | | | |
|--------------------|------------------|--------------------|------------------------|
| <u>(9/2) 571.8</u> | | <u>(9/2) 529.5</u> | |
| | | | <u>9/2 444.7</u> |
| <u>(7/2) 389.6</u> | | <u>7/2 325.0</u> | |
| | | <u>(5/2) 240.5</u> | <u>7/2 254.2</u> |
| | | <u>(5/2) 218.6</u> | <u>7/2+[404]</u> |
| <u>(3/2) 147.4</u> | | <u>5/2+[413]</u> | |
| <u>3/2+[411]</u> | <u>7/2 80.8</u> | | |
| | <u>5/2 0</u> | | $^{153}\text{Tb}_{88}$ |
| | <u>5/2+[402]</u> | | |

FIG. 5. Low-lying positive-parity levels in ^{153}Tb interpreted as members of bands based on Nilsson states. Spins in parentheses have not been fixed by the data but are consistent with experimental results.

the strength of the Coriolis interaction.

The Nilsson model³³ was used to generate single-particle energies and wave functions for the unmixed states.³⁴ The parameters of the Nilsson model were chosen initially according to the usual prescription as $\hbar\omega = 7.82$ MeV, $\kappa = 0.0647$, and $\mu = 0.592$. The deformation ϵ was chosen to be consistent with the experimental observation that the $\frac{3}{2}^+[411]$, $\frac{5}{2}^+[413]$, $\frac{5}{2}^+[402]$, and $\frac{7}{2}^+[404]$ bandheads lie within a 350-keV range. This restricts $\beta = 0.95\epsilon$ to a value between 0.1 and 0.2; the calculations reported below were carried out with $\beta = 0.15$. Though a value $\epsilon_4 = -0.04$ is suggested for well-deformed nuclei in this mass region, for simplicity we have taken $\epsilon_4 = 0$.

The values of $E(K)$ were obtained with $\Delta = 1.00$ MeV and $\lambda = 5.722\hbar\omega$. Under these conditions the $\frac{5}{2}^+[413]$ state lies lower than $\frac{5}{2}^+[402]$, in disagreement with the experimental observation. In the normal Nilsson scheme for protons, the $g_{7/2}$ shell-model state lies below the $d_{5/2}$ state. If the relative energy of the $d_{5/2}$ state is adjusted to lie 200 keV below the $g_{7/2}$ state, however, then the order of the $K = \frac{5}{2}^+$ bandheads agrees with experiment.

The systematic trend of the difference in $g_{7/2}$ - $d_{5/2}$ energies³⁵ is shown in Fig. 6 as a function of neutron number for $Z = 59, 61, \text{ and } 63$. For $Z = 65, N = 88$ it seems reasonable to expect the $d_{5/2}$ state to lie below the $g_{7/2}$ state. Hamamoto³⁶ has shown that a short-range neutron-proton interaction in the pairing model accounts for this trend. The reversal in order of the $d_{5/2}$ and $g_{7/2}$ states is equivalent to choosing μ as 0.48 (instead of 0.592). This is approximately the μ value for a 65-neutron system. The values of κ and μ are meant to describe a broad range of nuclei and are often adjusted for particular cases.³⁷ This modification is referred to below as the adjusted Nilsson model.

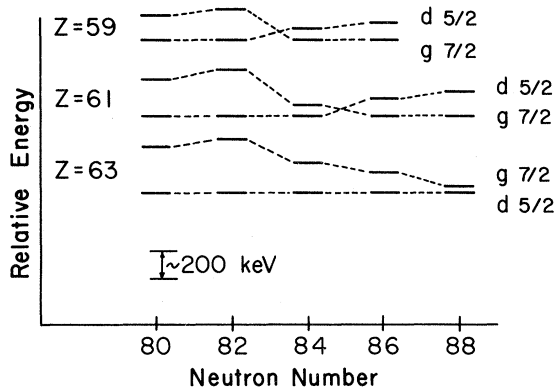


FIG. 6. Systematic trend of energies of $d_{5/2}$ and $g_{7/2}$ states in odd- Z nuclei. Experimental data are from Ref. 35.

The Coriolis-coupling calculation was done with the program BETABLE.³⁸ The $\frac{1}{2}^+[411]$, $\frac{3}{2}^+[411]$, $\frac{5}{2}^+[413]$, $\frac{5}{2}^+[402]$, and $\frac{7}{2}^+[404]$ bands were included in the mixing calculation. Matrix elements were obtained with the wave functions from the adjusted Nilsson model.³⁴ The decoupling parameter α for the $\frac{1}{2}^+[411]$ band was taken to be -1.217 keV. The variables of the calculation were $E(K)$ values of the $\frac{5}{2}^+[413]$, $\frac{5}{2}^+[402]$, and $\frac{7}{2}^+[404]$ orbitals, A (same for all bands), and $A'(K, K+1)$. The $E(K)$ values of the $\frac{1}{2}^+[411]$ and $\frac{3}{2}^+[411]$ orbitals were those obtained from the adjusted Nilsson model, 700 and 250 keV, respectively. The $E(K)$ values of the remaining orbitals were obtained by fitting. However, the resulting energies were only slightly different from those resulting from the adjusted Nilsson model (value given in parentheses): $\frac{5}{2}^+[413]$, 210(150) keV; $\frac{5}{2}^+[402]$, 120(100) keV; and $\frac{7}{2}^+[404]$, 300(200) keV.

Values of A and $A'(K, K+1)$ which provide reasonable fits to the experimental data are summarized in Table VI. The value of A for ^{153}Tb is larger than that for ^{155}Tb (12 keV for positive-parity bands),²⁵ consistent with ^{153}Tb having a smaller deformation and moment of inertia. The A' values are generally similar to those found for negative-parity states in ^{155}Tb (A'/A values in the range 0.53 to 1.03).²⁵

In Table VII are summarized the energies and mixing amplitudes of wave functions resulting from the calculation. The agreement of calculated level energies with experimental values is adequate. While bandhead states remain reasonably pure, higher members are strongly mixed, especially among members of the $\frac{5}{2}^+[413]$ and $\frac{7}{2}^+[404]$ bands. The mixing amplitudes indicate that the 254.2-keV state is primarily $\frac{7}{2}^+[404]$ and the 325.0-keV state is predominantly $\frac{7}{2}^+[\frac{7}{2}, \frac{5}{2}][413]$; the identification of states in Fig. 3 designates only the principal component of the wave function.

TABLE VI. Values of the inertial constant $A = \hbar^2/2\mathcal{I}$ and the Coriolis-coupling constant $A'(K, K+1)$. The $K = \frac{5}{2}^+$ states $\frac{5}{2}^+[413]$ and $\frac{5}{2}^+[402]$ are identified as $\frac{5}{2}$ and $\frac{5}{2}'$, respectively.

| Quantity | Value (keV) |
|---------------------------------|-------------|
| A | 17.8 |
| $A'(\frac{1}{2}, \frac{3}{2})$ | 12.0 |
| $A'(\frac{3}{2}, \frac{5}{2})$ | 2.0 |
| $A'(\frac{3}{2}, \frac{5}{2}')$ | 12.0 |
| $A'(\frac{5}{2}, \frac{7}{2})$ | 6.0 |
| $A'(\frac{5}{2}', \frac{7}{2})$ | 21.7 |

TABLE VII. Properties of Coriolis-mixed positive-parity states in ^{153}Tb .

| Energy (keV) | | Spin | | Mixing amplitudes | | | | |
|--------------|--------|--------------------------------------------------------|---------------|--------------------|--------------------|--------------------|--------------------|--------------------|
| Exp. | Theory | Exp. ^a | Theory | $\frac{1}{2}[411]$ | $\frac{3}{2}[411]$ | $\frac{5}{2}[413]$ | $\frac{5}{2}[402]$ | $\frac{7}{2}[404]$ |
| 0 | 0 | $\frac{5}{2}$ | $\frac{5}{2}$ | -0.002 | 0.235 | -0.003 | 0.972 | |
| 80.8 | 82.7 | $\frac{7}{2}$ | $\frac{7}{2}$ | 0.003 | -0.292 | 0.047 | -0.897 | 0.327 |
| 147.4 | 151.5 | $\frac{3}{2}(\frac{5}{2}, \frac{7}{2})$ | $\frac{3}{2}$ | -0.007 | 1.000 | | | |
| 240.5 | 255.7 | $\frac{5}{2}(\frac{7}{2})$ | $\frac{5}{2}$ | -0.010 | 0.971 | 0.055 | -0.234 | |
| 389.6 | 403.0 | $(\frac{5}{2}, \frac{7}{2})$ | $\frac{7}{2}$ | -0.018 | 0.912 | 0.140 | -0.349 | -0.163 |
| 571.8 | 591.6 | $(\frac{3}{2}, \frac{5}{2}, \frac{7}{2}, \frac{9}{2})$ | $\frac{9}{2}$ | 0.015 | -0.843 | -0.193 | 0.427 | 0.263 |
| 218.6 | 218.9 | $\frac{5}{2}(\frac{7}{2})$ | $\frac{5}{2}$ | 0.001 | -0.053 | 0.998 | 0.015 | |
| 325.0 | 353.4 | $\frac{7}{2}$ | $\frac{7}{2}$ | -0.003 | 0.197 | -0.932 | -0.001 | 0.305 |
| 529.5 | 523.5 | $\frac{9}{2}(\frac{5}{2}, \frac{7}{2})$ | $\frac{9}{2}$ | -0.005 | 0.309 | -0.872 | -0.018 | 0.380 |
| 254.2 | 260.5 | $\frac{7}{2}$ | $\frac{7}{2}$ | -0.003 | 0.210 | 0.332 | 0.269 | 0.879 |
| 444.7 | 416.5 | $\frac{9}{2}$ | $\frac{9}{2}$ | -0.004 | 0.294 | 0.444 | 0.291 | 0.794 |

^aValues in parentheses are formally allowed by the data but are considered less likely.

The mixed wave functions have been used to calculate relative $B(M1)$ values for a number of transitions which experimentally appear to be $M1$, or for mixed $M1/E2$ transitions in which a reasonably accurate correction could be made for an $E2$ component. These values are listed in Table VIII. Also shown are $B(M1)$ values calculated if the states are assumed to be unmixed. When mixing is taken into account, the agreement between theory and experiment is generally reasonable. In one case, however, the calculated and experimental values significantly disagree. This case involves the de-excitation of the 254.2-keV state. The calculated value is very sensitive to the [402] amplitude

TABLE VIII. $B(M1)$ ratios for deexcitation of positive-parity states in ^{153}Tb using Coriolis-mixed and unmixed wave functions.

| Initial state (keV) | Final states | | Expt. ^a | Theory | |
|---------------------|--------------|---------|--------------------|--------|-----------------------|
| | 1 (keV) | 2 (keV) | | Mixed | Unmixed ^b |
| 325.0 | 0 | 254.2 | 0.09 ± 0.02 | 0.15 | 0.11 |
| 325.0 | 80.8 | 254.2 | 0.60 ± 0.12 | 0.56 | 0.20 |
| 254.2 | 80.8 | 0 | 0.13 ± 0.01 | 1.70 | 0.30 |
| 389.6 | 240.5 | 0 | 10 ± 1 | 6 | 19 |
| 389.6 | 80.8 | 0 | 0.4 ± 0.1 | 5.0 | 10.6 |
| 571.8 | 389.6 | 254.2 | 9.0 ± 0.9 | 8.7 | ∞ ^c |

^aValues listed are the ratios $B(M1, \text{initial state} \rightarrow \text{final state 1})/B(M1, \text{initial state} \rightarrow \text{final state 2})$.

^bThe wave function for a state was taken to be entirely that of the state with the largest amplitude (see Table VII).

^cThe transition in the denominator is $\frac{9}{2}, \frac{3}{2}[411] \rightarrow \frac{7}{2}[404]$ which is forbidden by $M1$ for the unmixed state.

which dominates the transition probability. The experimental data may indicate that the [402] component in the wave function of the 254.2-keV state is much smaller than that resulting from the Coriolis mixing calculation. As a whole, however, the $B(M1)$ values provide support for a quasirotational description of positive-parity states in ^{153}Tb .

C. Possible vibration-coupled states

The states at 543.5, 630.4, 651.7, 660.1, 726.9, and 740.8 keV probably result from vibrations coupled to the quasiparticle Nilsson states. Both β - and γ -vibrational states have been reported in ^{155}Tb and ^{157}Tb with bandhead energies of 600–700 keV.^{23–25} The decay patterns of the states in ^{153}Tb indicate highly mixed configurations. For example, the 543.5-keV state decays to states in three different bands, while the 651.7- and 726.9-keV states decay to states in two bands as well as to the negative-parity state at 213.8 keV. The states at 630.4 and 660.1 keV may be somewhat purer; they populate predominantly only members of the $\frac{7}{2}^+[404]$ band. The 740.8-keV state deexcites mainly to $\frac{7}{2}^+$ members of both the $\frac{5}{2}^+[413]$ and $\frac{5}{2}^+[402]$ bands. In the latter transition, the conversion coefficient is significantly larger than that for $M1$, suggesting the presence of an $E0$ component. Thus the 740.8-keV state could have a major component arising from a β vibration coupled to the ground state.

A β -vibrational band built on the $\frac{3}{2}^+[411]$ state was proposed in Ref. 5. They assign the $\frac{5}{2}^+$ member at 799.9 keV and the $\frac{7}{2}^+$ member at 1076.1 keV. They report a 559.4-keV transition to the $\frac{5}{2}^+$ 240.5-keV state from the 799.9-keV state with an

$E0$ component. This transition is not observed in either our γ -ray or conversion-electron spectra. We observe instead a coincidence-confirmed $M1$ transition connecting the 799.9-keV state to the negative-parity state at 537.5 keV. Thus the state at 799.9 keV has negative parity. The 1087.1-keV state of Ref. 5 is reported to deexcite to the 389.6-keV state by a 697.4-keV transition with an $E0$ component. While we observe a 697.4-keV transition, our coincidence data eliminate the possibility of it populating the 389.6-keV state. Our conversion-electron spectra indicate that the intensity of the K -conversion line from the 697.4-keV transition must be at least a factor of 3 smaller than the value reported in Ref. 5.

D. Negative-parity states in ^{153}Tb

The low-lying negative-parity states, unlike the positive-parity states, are not analogs of similar states of the more deformed Tb nuclei. However, they can be accounted for in the rotational interpretation. According to Stephens,³² if the Fermi surface lies low in a high- j unique-parity shell-model orbital, at small prolate deformations ($\beta \lesssim 0.2$) the rotational bands originating from that orbital are so distorted by the Coriolis force that a new coupling scheme develops. The lowest-lying state will have a spin equal to the j value of the shell-model state, and the order and spacing of other spin states will depend on the actual values of β , λ , and the moment of inertia of the even-even core. This coupling scheme is viewed as resulting from an alignment of the motion of the odd particle with the rotation of the core and is generally referred to as the rotation-alignment model.

Since the negative-parity states in ^{153}Tb arise from the high- j unique-parity $h_{11/2}$ state, a calculation in the framework of the rotation-alignment model³² has been performed. This calculation is formally the same as that for the positive-parity states, except that every Nilsson state from the $h_{11/2}$ shell must be included in the diagonalization of the matrices whose elements are determined by Eqs. (1) and (3). The same values of β , λ , and Δ used for the positive-parity states were used for the negative-parity states. In the rotation-alignment model, $\hbar^2/2\mathcal{I}$ is determined by the even-even core. It was taken to be $\frac{1}{6}$ of the energy of the first excited 2^+ state (344 keV) in ^{152}Gd , which should approximately represent the core for ^{153}Tb . The parameter $A'(K, K+1)$ was taken to be equal to A ($\hbar^2/2\mathcal{I} = 57$ keV) in one calculation. In another calculation, A and $A'(K, K+1)$ were varied to fit the energies of the $\frac{11}{2}^-$ 163.3-keV state, the $\frac{7}{2}^-$ 213.8-keV state, the $\frac{9}{2}^-$ 263.0-keV state, and the state at 537.5 keV. This state was as-

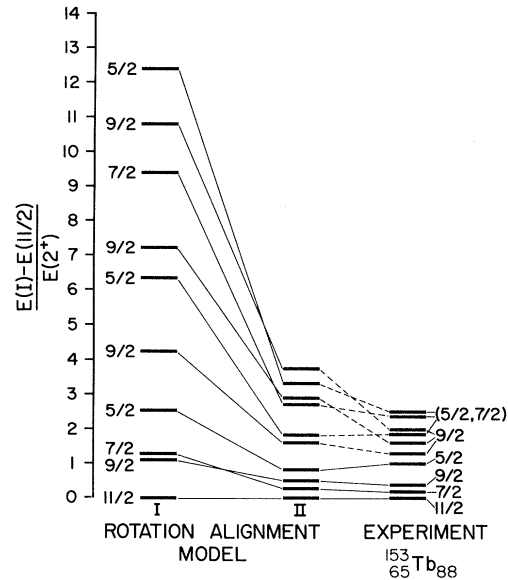


FIG. 7. Low-lying negative-parity levels in ^{153}Tb compared with the predictions of the rotation-alignment model. In Calculation I, no parameters were allowed to vary; in II, the parameters A and $A'(K, K+1)$ were allowed to vary (see text). The ordinate is the energy of a negative-parity level relative to the $\frac{11}{2}^-$ level at 163.3 keV in units of the energy of the 2^+ level in ^{152}Gd (344 keV). The correspondence between calculated higher-lying levels and experimental levels has not been established.

sumed to be $\frac{5}{2}^-$, which is consistent with the experimental data.

The results of these two calculations are shown in Fig. 7, where the calculation labeled I is with $A = A'(K, K+1) = 57$ keV, and the one labeled II is with A and $A'(K, K+1)$ treated as variables. In both calculations the same value of $A'(K, K+1)$ was used for each off-diagonal element. Calculation I, in which no parameters have been fitted, is in qualitative agreement with the experimental results; both spins and level order are reasonably well reproduced but the level spacing is too large. For the two-parameter fit, calculation II, the fitted values were $A = 20$ keV and $A'(K, K+1) = 18$ keV. These are physically reasonable values for the parameters, and considerable improvement in the fit, relative to calculation I, is obtained. The negative-parity states in ^{153}Tb are at least qualitatively consistent with the predictions of the rotation-alignment model.

The rotation-alignment-model calculation predicts that a series of high-spin states, known as a decoupled band, should also be present in ^{153}Tb . Preliminary results³⁹ of $(\alpha, xn\gamma)$ studies of high-spin states in ^{153}Tb tend to confirm these predictions of the calculation as well.

V. SUMMARY AND CONCLUSIONS

The decay of ^{153}Dy populates at least 54 levels in ^{153}Tb . Below 1 MeV, 20 states have positive parity, 10 negative, and for 3 others the parity is not known. In order to interpret such a complex level scheme in the framework of a relatively simple model with clear physical assumptions, we have used the conventional formalism for deformed nuclei—the particle-plus-rotor model with Coriolis mixing—to describe the positive-parity states. Though the ground state of an 88-neutron nucleus might not be expected to be stably deformed, the experimental energies and transition probabilities are reasonably reproduced for a deformation $\beta = 0.15$. Low-lying negative-parity states in ^{153}Tb are accounted for within the context of the rotation-alignment model in which the values of parameters that reproduce the level order correspond to weak prolate deformation. The β -decay transition prob-

abilities for populating the $\frac{5}{2}^+$ ground state and $\frac{7}{2}^+$ first excited state correspond to the values expected for members of a $K = \frac{5}{2}$ band.

The experimental data obtained in this work are consistent with the notion that ^{153}Tb is a weakly deformed nucleus. Many of the properties of low-lying states can be interpreted in this way.

ACKNOWLEDGMENTS

The interpretation of the experimental data in the context of several theoretical models would not have been possible without the advice, guidance, and computer codes of Teruo Kishimoto. We acknowledge also valuable discussions about nuclear theory with Chin W. Ma and P. K. Bindal. We are grateful for the assistance of D. R. Zolnowski, D. R. Haenni, M. B. Hughes, and J. L. Hunt in obtaining and analyzing the experimental data. F. M. Bernthal provided the Coriolis code BETABLE.

[†]Supported in part by the Robert A. Welch Foundation and the U.S. Energy Research and Development Administration.

*Present address: College of Medicine, Texas A&M University, College Station, Texas 77843.

¹For example, H. Beuscher, W. F. Davidson, R. M. Lieder, C. Mayer-Böricke, and H. Ihle, *Z. Phys.* **263**, 201 (1973); D. R. Zolnowski, T. Kishimoto, Y. Gono, and T. T. Sugihara, *Phys. Lett.* **55B**, 453 (1975).

²For example, H. J. Smith, D. G. Burke, M. W. Johns, G. Løvholden, and J. C. Waddington, *Phys. Rev. Lett.* **31**, 944 (1973); P. Kleinheinz, R. K. Sheline, M. R. Maier, R. M. Diamond, and F. S. Stephens, *ibid.* **32**, 68 (1974).

³J. S. Boyno and J. R. Huizenga, *Phys. Rev. C* **6**, 1411 (1972); J. C. Tippet and D. G. Burke, *Can. J. Phys.* **50**, 3152 (1972).

⁴B. Harmatz and T. H. Handley, *Nucl. Phys.* **A191**, 497 (1972).

⁵K. Zuber, Ts. Vylov, I. I. Gromova, Ya. Zuber, H.-G. Ortlepp, and N. A. Lebedev, Dubna Report No. P6-8669, 1975 (unpublished).

⁶O. Straume, G. Løvholden, and D. G. Burke, *Nucl. Phys.* **A266**, 390 (1976).

⁷D. G. Burke, G. Løvholden, and J. C. Waddington, *Phys. Lett.* **43B**, 470 (1973); H. Taketani, H. L. Sharma, and N. M. Hintz, *Phys. Rev. C* **12**, 108 (1975).

⁸D. R. Haenni, Ph.D. dissertation, Texas A&M University, 1975 (unpublished).

⁹A. H. Wapstra and N. B. Gove, *Nucl. Data* **A9**, 268 (1971).

¹⁰G. T. Garvey, W. J. Gerace, R. L. Jaffe, I. Talmi, and I. Kelson, *Rev. Mod. Phys.* **41**, 51 (1969).

¹¹D. R. Zolnowski and T. T. Sugihara, *Nucl. Instrum. Methods* **114**, 341 (1974).

¹²R. S. Hager and E. C. Seltzer, *Nucl. Data* **A4**, 1 (1968).

¹³V. T. Gritsyna and H. H. Forester, *Nucl. Phys.* **61**,

129 (1965).

¹⁴K. E. Ädelroth, H. Hyqvist, and A. Rosen, *Phys. Scr.* **2**, 96 (1970).

¹⁵A. Rosen, C. Ekström, H. Hyqvist, and K. E. Ädelroth, *Nucl. Phys.* **A154**, 283 (1970).

¹⁶J. W. Ford, A. V. Ramayya, and J. J. Pinajian, *Nucl. Phys.* **A146**, 397 (1970); J. E. Thun and T. R. Miller, *ibid.* **A193**, 337 (1972).

¹⁷A. Bäcklin, S. G. Malmskog, and H. Solhed, *Ark. Fys.* **34**, 495 (1966).

¹⁸T. Kishimoto, private communication.

¹⁹M. A. Preston, *Physics of the Nucleus* (Addison-Wesley, Reading, Massachusetts, 1962), p. 451.

²⁰E. J. Konopinski, *The Theory of Radioactivity* (Oxford U.P., Oxford, 1966); we thank Professor C. W. Ma for making this calculation for us.

²¹R. E. Eppley, W. C. McHarris, and W. H. Kelly, *Phys. Rev. C* **2**, 1077 (1970).

²²L. Funke, H. Graber, K. H. Kaun, H. Sodan, and L. Werner, *Nucl. Phys.* **74**, 145 (1965).

²³G. G. Seaman, E. M. Bernstein, and J. M. Palms, *Phys. Rev.* **161**, 1223 (1967).

²⁴P. H. Blichert-Toft, E. G. Funk, and J. W. Mihelich, *Nucl. Phys.* **A100**, 369 (1967); J. L. Barat and J. Tréherne, *ibid.* **A199**, 386 (1973).

²⁵G. Winter, L. Funke, K. H. Kaun, P. Kemnitz, and H. Sodan, *Nucl. Phys.* **A176**, 609 (1971).

²⁶E. Browne and F. R. Femenia, *Nucl. Data* **A10**, 81 (1971).

²⁷T. Tuurnala, A. Siivola, P. Jartti, and T. Liljavirta, *Z. Phys.* **266**, 103 (1974).

²⁸G. Løvholden and D. G. Burke, *Can. J. Phys.* **51**, 2354 (1973).

²⁹M. E. Bunker and C. W. Reich, *Rev. Mod. Phys.* **43**, 348 (1971).

³⁰P. Alexander, F. Boehm, and E. Kankeleit, *Phys. Rev.* **133**, B284 (1964).

³¹M. A. Preston (see Ref. 19), p. 259.

- ³²F. S. Stephens, *Rev. Mod. Phys.* 47, 43 (1975).
- ³³S. G. Nilsson, C. F. Tsang, A. Sobiczewski, Z. Szymanski, S. Wycech, C. Gustafson, I.-L. Lamm, P. Möller, and B. Nilsson, *Nucl. Phys.* A131, 1 (1969).
- ³⁴The program VIBDEF by T. Kishimoto was used to calculate Nilsson wave functions and matrix elements.
- ³⁵ $A=137$: D. Habs *et al.*, in *Proceedings of the International Conference on Nuclear Physics*, edited by J. deBoer and H. J. Mang (North-Holland, Amsterdam/American Elsevier, New York, 1973), p. 183; $A=139$: L. R. Greenwood, *Nucl. Data* B12, 139 (1974); $A=141$: R. L. Auble, *ibid.* 10, 151 (1973); $A=143$: L. W. Chiao and S. Raman, *ibid.* B2-1, 25 (1967); D. Habs (see above); $A=145$: L. W. Chiao and M. J. Martin, *Nucl. Data* B2-1, 81 (1967); K. S. Toth, C. B. Bingham, and W.-D. Schmidt-Ott, *Phys. Rev. C* 6, 2550 (1974); $A=147$: W. B. Ewbank, M. J. Martin, and S. Raman, *Nucl. Data* B2-4, 35 (1967); $A=149$: Refs. 17 and 21.
- ³⁶I. Hamamoto, *Nucl. Phys.* 86, 208 (1966).
- ³⁷I. Hamamoto and T. Udagawa, *Nucl. Phys.* A126, 241 (1969).
- ³⁸We are indebted to Professor F. M. Bernthal for providing this program.
- ³⁹M. D. Devous, T. Kishimoto, and T. T. Sugihara, *Bull. Am. Phys. Soc.* 20, 1189 (1975).